Analysis of the Origin of Landslides in the New Madrid Seismic Zone

U.S. GEOLOGICAL SURVEY PROFESSIONAL PAPER 1538–D

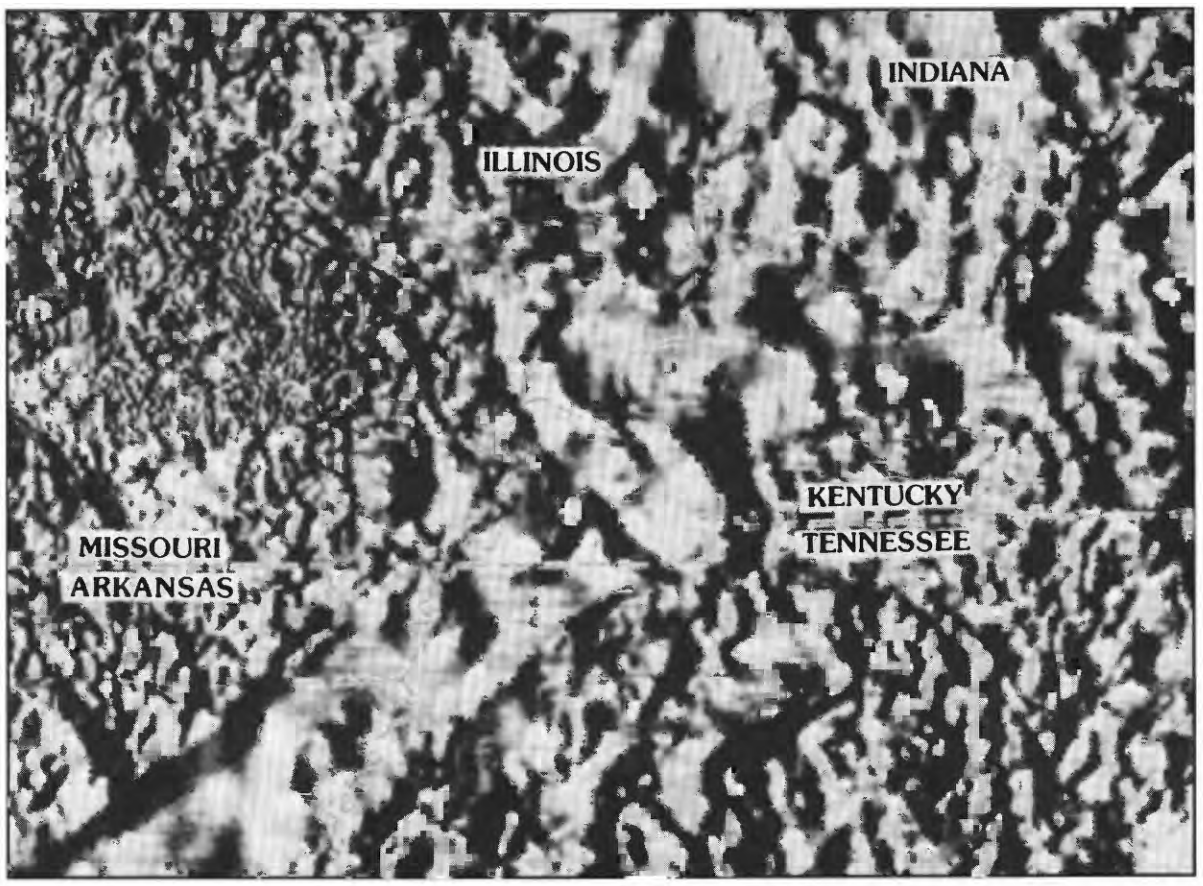

Cover. Part of a gray, shaded-relief, reduced-to-pole magnetic anomaly map. Map area includes parts of Missouri, Illinois, Indiana, Kentucky, Tennessee, and Arkansas. Illumination is from the west. Figure is from *Geophysical setting of the Reelfoot rift and relations between rift structures and the New Madrid seismic zone*, by Thomas G. Hildenbrand and John D. Hendricks (chapter E in this series).

Analysis of the Origin of Landslides in the New Madrid Seismic Zone

By Randall W. Jibson *and* David K. Keefer

INVESTIGATIONS OF THE NEW MADRID SEISMIC ZONE
Edited by Kaye M. Shedlock *and* Arch C. Johnston

U.S. GEOLOGICAL SURVEY PROFESSIONAL PAPER 1538–D

UNITED STATES GOVERNMENT PRINTING OFFICE, WASHINGTON : 1994

U.S. DEPARTMENT OF THE INTERIOR
BRUCE BABBITT, Secretary

U.S. GEOLOGICAL SURVEY
Robert M. Hirsch, Acting Director

For Sale by U.S. Geological Survey, Map Distribution
Box 25286, MS 306, Federal Center
Denver, CO 80225

Library of Congress Cataloging-in-Publication Data

Jibson, Randall W.
Analysis of the origin of landslides in the New Madrid seismic zone / by Randall W. Jibson and David K. Keefer.
p. cm.—(Investigations of the New Madrid seismic zone ; D)(U.S. Geological Survey professional paper ; 1538)
Includes bibliographic references.
Supt. of Docs. no.: I 19.16 : 1538D
1. Landslides—Missouri—New Madrid Region. I. Keefer, David K. II. Title. III. Series. IV. Series: U.S. Geological Survey professional paper ; 1538.
QE535.2.U6I59 1994 vol. D
[QE 599.U5]
551.2'2'0 9778985—dc20 93–38068
[551.3'07] CIP

CONTENTS

Abstract D1
Introduction 1
Geologic Setting 2
Seismic History 3
Description of Landslides in the Area 3
Previous Work 4
Analysis of the Stewart and Campbell Landslides 5
  Geotechnical Investigation 7
  Static (Aseismic) Slope Stability Analysis 8
    Idealized Pre-Landslide Bluff Model 8
    Ground-Water Conditions 8
    Method of Stability Analysis 9
    Results of Static Slope Stability Analysis 10
  Dynamic (Seismic) Slope Stability Analysis 11
    Factor of Safety 12
    Thrust Angle 14
    Earthquake Acceleration-Time History 15
    Calculation of the Newmark Landslide Displacement 17
    Results of Dynamic Analysis of Stewart Landslide 18
    Results of Dynamic Analysis of Campbell Landslide 18
  Summary of Stability Analyses 18
What if Seismic Conditions Are Unknown? 18
Discussion 20
Summary and Conclusions 21
References Cited 22

FIGURES

1. Map showing location of the study area D2
2. Isoseismal map of the 1811–12 New Madrid earthquakes 4
3. Idealized drawings of landslides along bluffs in study area 5
4. Map showing major features of the Stewart landslide 6
5. Profile of Stewart landslide 6
6. Map of part of the Campbell earth-flow complex near the line of profile 7
7. Profile of Campbell landslide 7
8. Idealized model of bluff at Stewart site in drained conditions 8
9. Idealized model of bluff at Campbell site in drained conditions 9
10. Ground-water conditions modeled in the slope stability analysis 9
11. Factor of safety versus water-table level at the Stewart site 10
12. Factor of safety versus water-table level at the Campbell site 11
13. Critical slip surfaces in drained conditions at the Stewart site 11
14. Critical slip surfaces in drained conditions at the Campbell site 12
15. Demonstration of the Newmark-analysis algorithm 12

16. Idealized model of bluff at Stewart site in undrained conditions D13
17. Idealized model of bluff at Campbell site in undrained conditions 13
18. Critical slip surfaces in undrained conditions at the Stewart site 14
19. Critical slip surfaces in undrained conditions at the Campbell site 15
20. Newmark displacement as a function of Arias intensity for critical accelerations of 0.02–0.40 *g* 19
21. Critical acceleration contours from multivariate regression of Arias intensity and critical acceleration versus Newmark displacement 19

TABLES

1. Drained factors of safety from the Stewart and Campbell landslides D10
2. Undrained factors of safety from the Stewart and Campbell landslides 14
3. Strong-motion records used to model 1811–12 ground shaking 16
4. Strong-motion records selected for analysis 19
5. Most damaging earthquakes since 1811–12 20

ANALYSIS OF THE ORIGIN OF LANDSLIDES IN THE NEW MADRID SEISMIC ZONE

By Randall W. Jibson[1] *and* David K. Keefer[2]

ABSTRACT

We develop a method for determining if a landslide or group of landslides of unknown origin was triggered by earthquake shaking. Important applications of this method are in seismic-hazard analysis and paleoseismology. If a group of landslides in a region can be shown to be statically stable but dynamically unstable, an earthquake origin can be inferred and the minimum shaking intensity required to have caused failure can be estimated. If such landslide features can be dated, a date for the triggering earthquake can be ascertained.

We analyze two landslides in the New Madrid seismic zone that represent the types of landslide features that previous research suggests may have been triggered by the 1811–12 earthquakes. Slope stability models of aseismic conditions show that neither slide could have formed aseismically even in unrealistically high ground-water conditions. Dynamic stability analysis using Newmark's method shows that both slides would have experienced large inertial displacements during earthquake shaking similar to that which occurred in 1811–12; these displacements are large enough that catastrophic failure would result. Thus, these landslides probably formed during the 1811–12 earthquakes.

Our analysis yields a general relationship between Newmark landslide displacement, earthquake shaking intensity, and the critical acceleration of a landslide. Using this relationship, we estimate the minimum shaking intensities required to trigger the types of landslides studied. Results indicate that an m_b=5.8 or M=5.9 earthquake is the lower bound threshold at zero epicentral distance that could trigger catastrophic movement of typical block slides in the New Madrid seismic zone; for earth flows, m_b=5.4 or M=5.3 is the threshold earthquake. This approach can be applied in seismic-hazard analyses elsewhere to determine regional seismic slope stability.

INTRODUCTION

Among the most dramatic effects of the New Madrid earthquakes of 1811–12 were the numerous landslides along the bluffs bordering the Mississippi alluvial plain in western Tennessee and Kentucky. In his report of a field investigation of the New Madrid earthquakes conducted in 1904, Fuller (1912, p. 59) stated:

> Probably no feature of the earthquake is more striking than the landslides developed in certain of the steeper bluffs * * *. From the vicinity of Hickman in southwestern Kentucky at least to the mouth of the Obion River, about halfway across the state of Tennessee * * * the landslides are a striking feature. Skirting the edge of the bluffs, in the vicinity of Reelfoot Lake, a characteristic landslide topography is almost constantly in sight * * *.

Many landslide features are currently visible along the bluffs in the epicentral area of the 1811–12 earthquakes, but determining which, if any, of these features were triggered in 1811–12 is a complex and difficult problem. In our recent studies (Jibson and Keefer, 1988, 1989), described in more detail later, we analyzed field and historical data and the regional distribution of landslides in the epicentral area. The data and conclusions from these studies, which were based on a consideration of the entire group of landslides at a regional scale, are consistent with many of these landslides having been triggered by the 1811–12 earthquakes. In the present paper, we use slope stability analysis to demonstrate that two representative individual landslides in the epicentral area could have resulted only from strong earthquake shaking such as that generated in 1811–12 and not from any other cause, such as increased ground-water levels. A detailed analysis of the stability of these individual landslides provides a firmer basis for our interpretation of the ground-failure effects of the 1811–12 earthquakes and will help us predict the conditions necessary to trigger widespread landsliding in future earthquakes in the New Madrid seismic zone.

[1] U.S. Geological Survey, Mail Stop 966, P.O. Box 25046, Denver Federal Center, Lakewood, CO 80225.

[2] U.S. Geological Survey, Mail Stop 998, 345 Middlefield Rd., Menlo Park, CA 94025.

The successful application of the approach detailed in this paper also establishes a procedure for determining the probable cause of failure of landslides elsewhere. The ability to determine whether a landslide formed as a result of earthquake shaking or from other factors opens several opportunities for using landslide analysis to interpret the recent geologic record. For example, dating landslides that can be shown to have formed during earthquake shaking would be a valuable tool in paleoseismic studies, particularly in areas such as the Central United States, where surface exposures of seismogenic faults are rare or absent.

In this paper, we address a single fundamental question: Can we analyze a landslide of unknown origin and determine that (1) it could not have formed aseismically and (2) it must have formed as the result of earthquake shaking? To address this question, we review the geological and seismological context of the study, present the geotechnical data necessary for the analysis of the stability of the two representative landslides, and interpret the origin of these landslides in light of the results of the analyses. Further, we document and test a more general procedure for determining whether or not old landslides were triggered by earthquakes and propose a general quantitative relationship between earthquake shaking intensity and dynamic (seismic) slope stability.

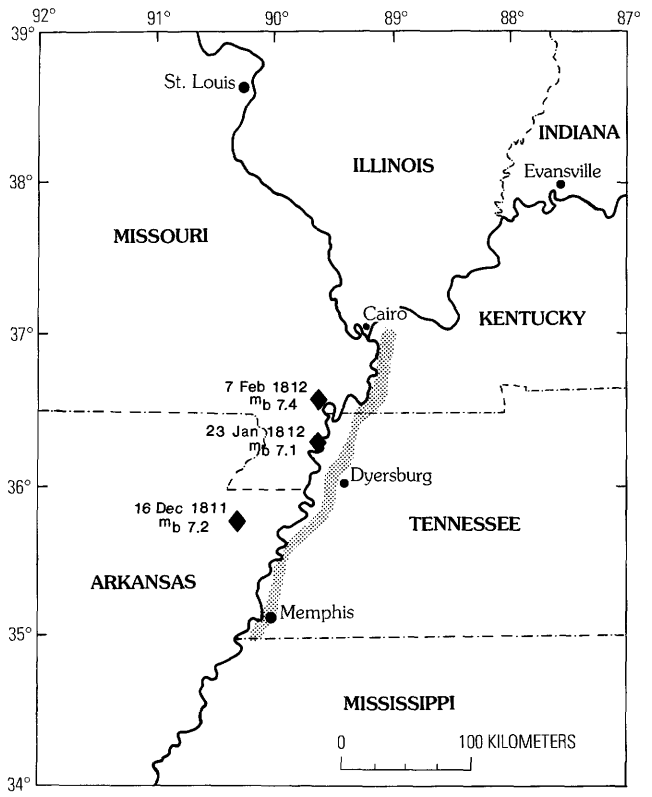

Figure 1. Study area (shaded) and estimated epicenters (diamonds), dates, and estimated body-wave magnitudes (m_b) of the three largest earthquakes in the 1811–12 sequence (earthquake locations and magnitudes from Nuttli, 1983).

GEOLOGIC SETTING

The area affected by major landsliding during the 1811–12 earthquakes includes more than 300 km of bluffs forming the eastern edge of the Mississippi alluvial plain between Cairo, Ill., and Memphis, Tenn. (fig. 1). The bluffs are along the eastern flank of the northern Mississippi Embayment, a broad, south-southwest-plunging syncline whose axis roughly coincides with the Mississippi River. Embayment deposits exposed in the bluffs thus generally dip to the west-northwest in most of the area. The region is seismically active, as evidenced by the 1811–12 earthquake sequence and continuing seismicity.

The average height of the bluffs in this area is 35 m, though in some areas they are as high as 70 m. Bluff slope angles are from a few degrees to vertical; most are 15°–25°. The bluffs trend north-northeast, approximately parallel with the Mississippi River. Locally, however, the bluff line is sinuous where the river has eroded arcuate meander scars.

The Eocene Jackson Formation (Conrad, 1856) forms the base of the bluffs throughout most of the area. Exposures are as thick as 45 m in the bluffs. The composition of the Jackson Formation is highly variable, but it generally consists of discontinuous layers of shallow-marine embayment deposits of clay and silt ranging from a few centimeters to several meters thick. In some areas, the Jackson Formation contains clean, uncemented sand layers as thick as several meters interbedded with soft clay layers. The Eocene beds generally dip a few degrees west-northwest (out of the bluff face in most of the area), but the amount and direction of dip vary locally; the amount of dip is generally less than 20°. The unconformity on top of the Eocene section is highly irregular, but, in areas where it has been mapped, it approximately parallels the present ground surface.

Lying unconformably on the Jackson Formation is as much as 20 m of Pliocene terrace gravel and sand of the Lafayette Gravel (McGee, 1891; Potter, 1955). The gravel and sand lenses commonly are uncemented but at some localities contain concretionary beds as thick as 2 m. The Lafayette Gravel is locally saturated where water tables are perched, and it probably is subject to large seasonal fluctuations in ground-water conditions. The unit pinches out in some areas.

The bluffs are capped by 5–50 m of Pleistocene loess lying unconformably on the Lafayette Gravel and Jackson Formation. The average thickness of the loess in the area is about 15 m. Loess is glacially derived, eolian silt that commonly forms vertical faces owing to the presence of vertical fractures. Vertical slopes can be supported because the loess in the study area has cohesion imparted by a clay

binder, or calcareous cementation, or both (Krinitzsky and Turnbull, 1969).

SEISMIC HISTORY

The bluffs are in the epicentral region of the 1811–12 New Madrid earthquake sequence, the most severe seismic event in historical times in the Central and Eastern United States. The three largest events, which occurred on 16 December 1811, 23 January 1812, and 7 February 1812, had estimated magnitudes corresponding to 7.1–7.4 on the body-wave magnitude (m_b) scale (Nuttli, 1973) and 8.1–8.3 on the moment magnitude (M) scale (Hamilton and Johnston, 1990). Thousands of aftershocks shook the area for many months, several of which were at least of moderate intensity (Nuttli, 1973).

The effects of the 1811–12 earthquake sequence have been described by Fuller (1912), Nuttli (1973), and Stearns and Wilson (1972); liquefaction effects were further documented by Saucier (1977) and Obermeier (1989). Figure 2 is a composite isoseismal map of the sequence, based on the Modified Mercalli intensity (MMI) scale, compiled by Stearns and Wilson (1972). Immediately apparent is the large area affected by the earthquakes. Nuttli (1973) estimated that 2,500,000 km^2 was affected at MMI≥V, the threshold of structural damage, and that 600,000 km^2 was affected at MMI≥VII, the threshold of major damage. This compares to 150,000 km^2 affected at MMI≥V and 30,000 km^2 affected at MMI≥VII for the 1906 San Francisco earthquake, which had about the same magnitude. The 1811–12 earthquakes were felt as far away as Detroit (900 km), Toronto (1,200 km), New York City (1,400 km), and Boston (1,700 km); in all they were felt over more than 5,000,000 km^2 (Stearns and Wilson, 1972). In Washington, D.C. (1,100 km), people were awakened from sleep, dishes rattled, and suspended objects swung. Chimneys were damaged as far away as Richmond, Va. (1,100 km), Savannah, Ga. (1,000 km), and Cincinnati, Ohio (600 km); plaster cracked and fell in Columbia, S.C. (900 km); and many homes were badly damaged in St. Louis (250 km), all as a result of these earthquakes (Nuttli, 1973).

The epicentral area of greatest damage included approximately 130,000 km^2 (Fuller, 1912). Within this region, uplift and subsidence on the order of a few meters occurred over hundreds of square kilometers, the most notable area of subsidence being Reelfoot Lake in northwestern Tennessee. Also, fissuring of the ground surface, caving of river banks, and extrusion of huge quantities of sand and water from the subsurface occurred. The last effect was the result of liquefaction of sand layers and is estimated to have inundated approximately 10,000 km^2 with as much as 2 m of sand and water. More than 650 km^2 of timber was destroyed by flooding, violent ground shaking, or landsliding (Fuller, 1912). Eyewitness accounts describe the entire land surface as being disrupted and, in many places, uninhabitable (Penick, 1981). Pertinent to this study are reports of landslides along the bluffs in western Tennessee and Kentucky from Hickman, Ky., at least to the Obion River, near Dyersburg, Tenn. (Fuller, 1912).

DESCRIPTION OF LANDSLIDES IN THE AREA

Along the bluffs in the study area, 221 large (greater than 50 m wide) landslides were identified on air photos, examined on the ground, classified morphologically (after Varnes, 1978), and plotted on an inventory map (Jibson and Keefer, 1988). Three classes of landslides were mapped: old coherent slides, earth flows, and young rotational slumps.

Old coherent slides (fig. 3) constitute 65 percent of the landslides in the study area. This group includes translational (block) slides and rotational slides (slumps), both of which remained fairly intact or coherent. These slides are termed "old" because they all are eroded and revegetated and show no sign of activity for at least the past several decades. They all appear to be of similar age based primarily on amount of scarp retreat, degree of erosion of ridges, and vegetation density and age on scarps and disrupted areas (Jibson and Keefer, 1988). Translational and rotational slides were grouped together because heavy tree cover and eroded features generally made it impossible to distinguish between them. These landslides are deep seated (typically deeper than 20 m) and have basal shear surfaces in the clayey Jackson Formation that form the base of the bluffs. The translational block slides (fig. 3*A*) are characterized by horst-and-graben topography, and toe areas commonly have compressional ridges in front of the landslide blocks that moved down and out (as far as 100 m) from the parent slope. Basal shear surfaces dip 4°–25°. The old rotational slumps (fig. 3*B*) are characterized by either single or multiple blocks that generally appear to have rotated a large amount relative to the younger slumps described subsequently.

Earth flows (fig. 3*C*) constitute 24 percent of the landslides. Characteristic features are gently hummocky topography and ridges of accumulated material in the toe area. A few deforested earth-flow complexes contain recently (0–5 yr) active flows. The large majority of the earth flows, however, including all those on forested slopes, are eroded and revegetated and have been inactive for at least the past several decades. As with the old coherent slides, the degree of erosion and revegetation suggests similar ages for the earth flows (Jibson and Keefer, 1988).

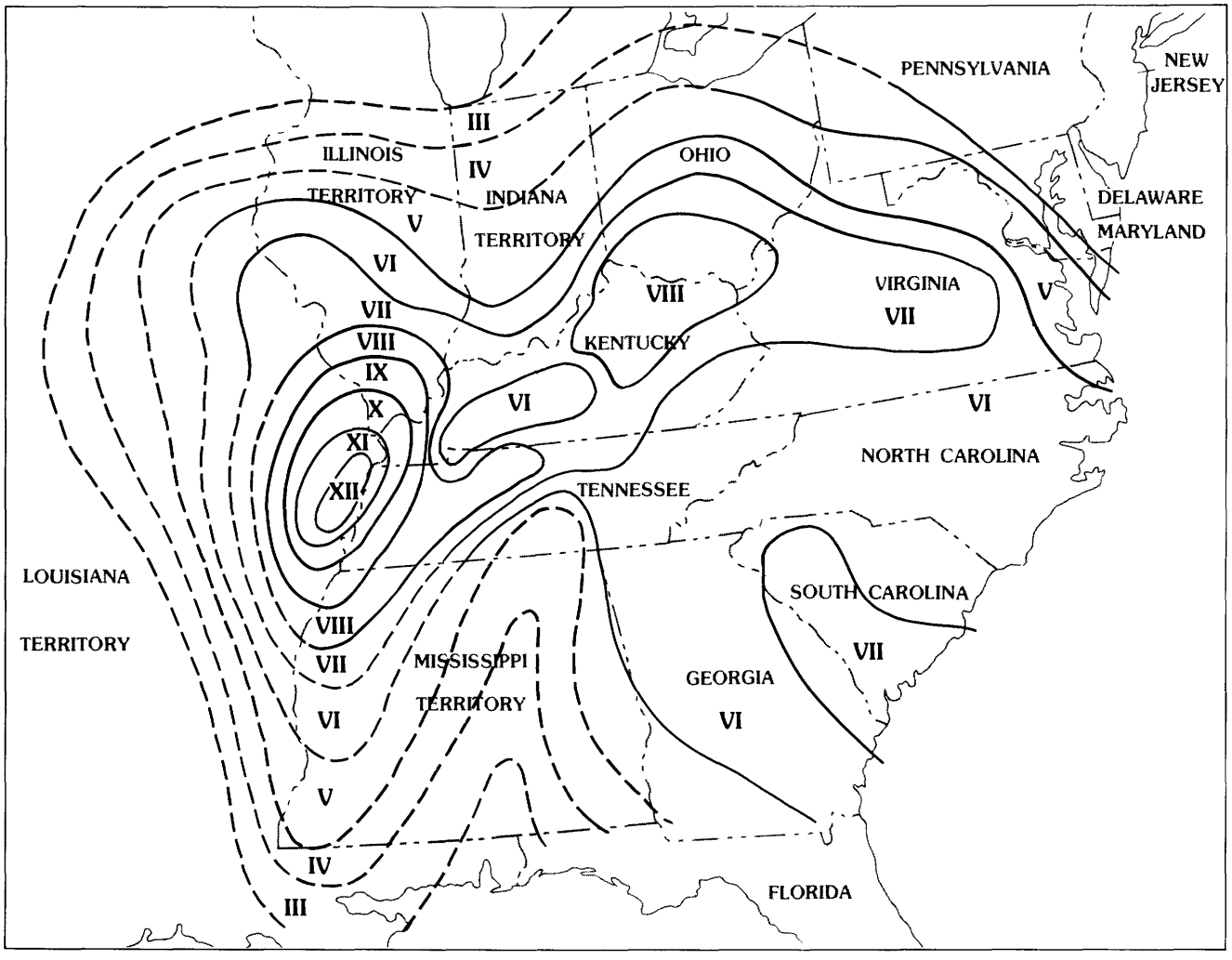

Figure 2. Composite isoseismal map of the 1811–12 New Madrid earthquake sequence showing maximum Modified Mercalli intensity values. Adapted from Stearns and Wilson (1972).

The remaining 11 percent of the landslides are young rotational slumps. Young slumps are present only along bluffs where the Mississippi River has impinged since 1820 (about 11 percent of bluff length). The young slumps are characterized by massive single slump blocks that form where the river has undercut the bluffs. They are differentiated from old slumps on the bases of less rotation, less scarp and head erosion, absence of multiple blocks, and, in some cases, absent or young vegetation (Jibson and Keefer, 1988).

PREVIOUS WORK

The two earliest field investigations of the landslides, conducted in 1891 (McGee, 1893) and 1904 (Fuller, 1912), suggest that at least some of the old coherent slides in part of the area formed during the 1811–12 earthquakes. More recent studies (Jibson and Keefer, 1984, 1988; Jibson, 1985) used dendrochronology, geomorphology, historical topographic maps, local historical accounts, and comparisons with landslides triggered by other earthquakes to show that the apparent ages and morphologies of most of the old coherent slides and earth flows are consistent with triggering during the 1811–12 earthquakes. The evidence further shows that the only ongoing, large, aseismic landslide activity in the area results from fluvial undercutting of near-river bluffs, which triggers slumps that are morphologically distinct from the old coherent slides on bluffs away from the river. Also, the landslides on bluffs away from the river all appear to be about the same age, which suggests a common triggering event; these landslides are unrelated to fluvial activity and have no active analogs in the area (Jibson and Keefer, 1988).

In a statistical analysis of the regional distribution of the three types of landslides along the bluffs, we (Jibson and Keefer, 1989) used discriminant analysis and multivariate linear regression to detect correlation between landslide distribution and slope height and steepness, strati-

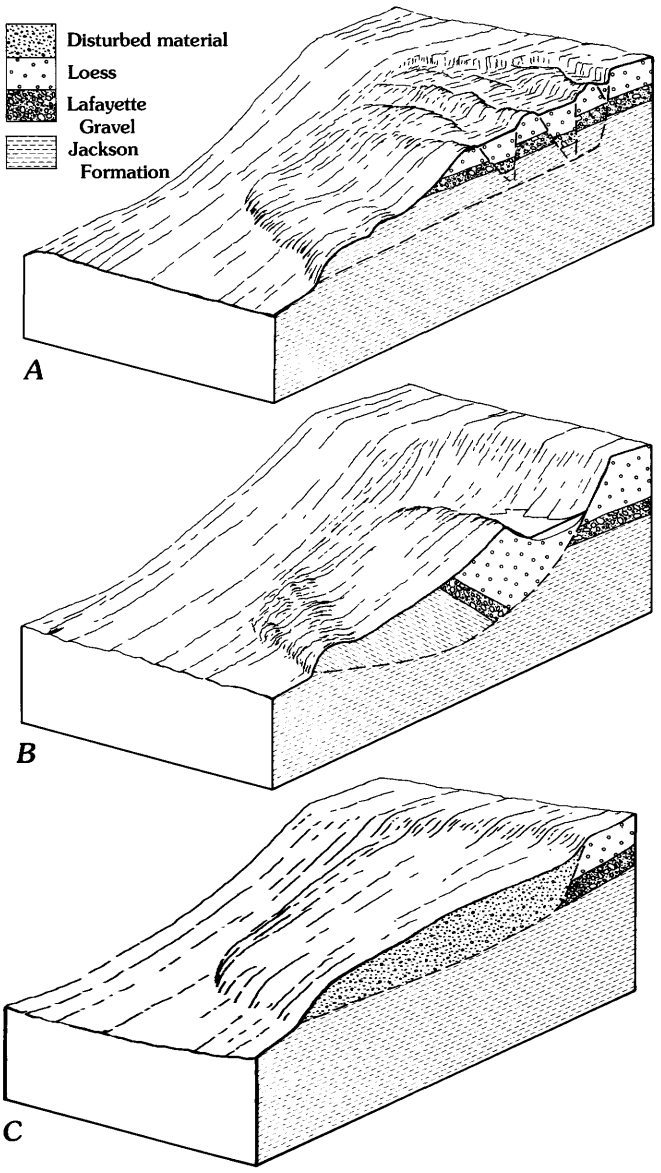

Figure 3. Idealized drawings of types of landslides along the bluffs. These landslides all have eroded, revegetated features, and no active analogs are present in the area. *A*, Old coherent translational block slide. *B*, Old coherent rotational slump. *C*, Earth flow.

graphic variation, slope aspect, and proximity to the hypocenters of the 1811–12 New Madrid earthquakes. The discriminant analysis shows no correlation between young rotational slumps and the earthquakes. Bluffs having old coherent slides and earth flows, however, are significantly closer to the estimated hypocenters of the 1811–12 earthquakes than bluffs without these slides (Jibson and Keefer, 1989). Multiple regression analysis, which simultaneously combined all the factors cited above, likewise indicates no correlation between the distribution of young rotational slumps and the earthquake locations. The distribution of old coherent slides and earth flows, however, strongly correlates with the proximity to the hypocenters of the 1811–12 earthquakes, as well as with slope height and aspect (Jibson and Keefer, 1989). The results of these statistical analyses thus show that the old coherent slides and earth flows in the area are spatially related to the 1811–12 earthquake hypocenters.

The methods and conclusions from these previous studies do not address the questions of whether any specific landslide in the area was actually triggered in 1811–12 or what conditions led to the failure of a given landslide. The following sections, based on more recent studies (Jibson and Keefer, 1992, 1993), describe an approach to address these questions.

ANALYSIS OF THE STEWART AND CAMPBELL LANDSLIDES

We chose two landslides for detailed analysis: the Stewart landslide, a translational block slide about 11 km north of Dyersburg, Tenn., and the Campbell landslide, an earth flow about 10 km west of Dyersburg (fig. 1). These slides are representative of the two major types of old landslides in the area that previous research indicates may have been triggered by the 1811–12 earthquakes.

The Stewart landslide averages 800 m wide by 400 m long and covers approximately 0.3 km^2. Large parts of the slide are heavily forested, which precludes detailed topographic mapping. Figure 4 is a sketch map of the landslide compiled using 1:24,000-scale topographic map contours, profiles measured in 2-m increments, 1:20,000-scale air photos, and field observations. Figure 5 shows a profile of the Stewart slide; subsurface data are from drilling along the line of profile. The broad, bowl-shaped scarp forms a notable reentrant in the local bluff line, and below the scarp several large horst-and-graben blocks form prominent but discontinuous ridges and troughs that interfinger with one another and create a complex topography. The grabens commonly have sloping bottoms that allow drainage; however, one ephemeral sag pond is in a closed depression on a graben block. Some of the smaller horst blocks show evidence of headward rotation of as much as 10°, but the larger blocks, as well as most of the smaller ones, did not rotate and apparently translated with little internal deformation on a gently sloping basal shear surface. The horst block shown on the profile (fig. 5), for example, is displaced downward only 3 m but moved horizontally about 50 m. Thus, the basal shear surface dips less than 4°. Below the main landslide blocks, a toe area of subdued, hummocky topography formed from subsidiary slumping from the displaced bluff face (fig. 5) and compression of the material at the base of the slope when the landslide blocks moved down and out from the parent slope.

The Campbell landslide is a large complex of coalescing earth flows that extends almost 4 km along the bluffs.

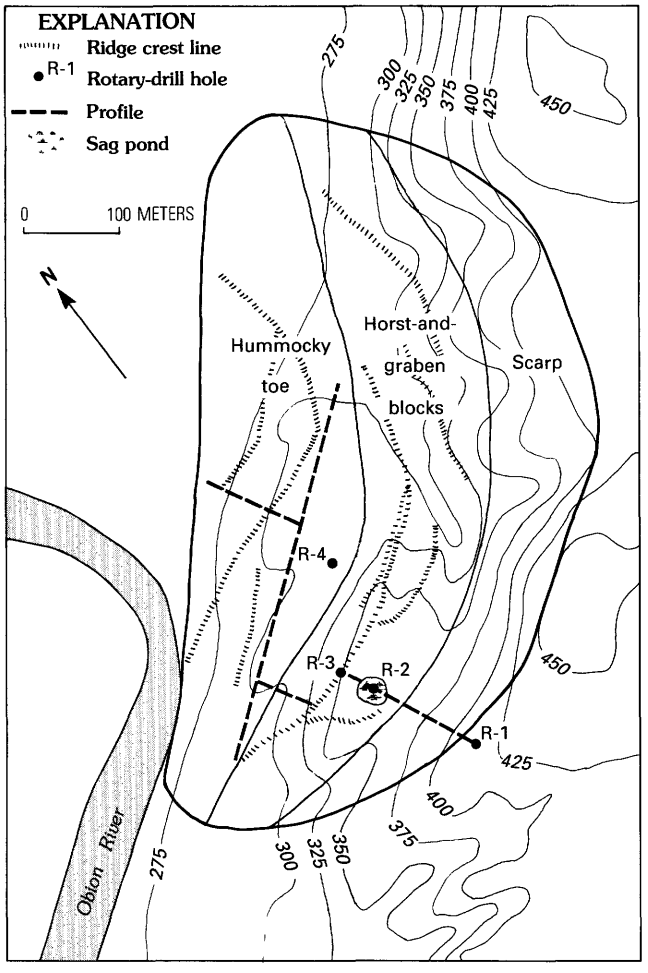

Figure 4. Map showing major features of the Stewart landslide. Contours in feet above mean sea level (1 ft = 0.305 m).

Heavy tree cover makes detailed mapping infeasible; a sketch map of the part of the complex near the line of profile is shown in figure 6, and a profile is shown in figure 7. Individual earth flows in the complex average about 400 m long, and the complex covers about 1.5 km^2.

The Campbell slide has subtle features: gently hummocky slopes, between 5° and 10°, lie downslope from a 20° scarp near the top of the bluff. Discreet lobes and an irregular scarp visible on air photos indicate that landsliding initiated at several localities and coalesced to form a continuous complex. All of these lobes appear to be the same age; no evidence exists of episodic movement on the slide except in deforested areas where smaller active earth flows are present (Jibson and Keefer, 1988). Along the base of the bluff, a gentle compressional ridge formed where material moved downslope to an area flat enough to inhibit movement and cause accumulation (fig. 7). Two lobes of material are visible in the profile; the break in slope between the toe and the head scarp is probably a secondary scarp. Some of the larger swales on the complex have been dammed for stock ponds, but no original sag ponds are present. The location of the disturbed zone in the drill holes (fig. 7) and the surface morphology of the slide indicate that sliding probably occurred along a shear surface that dips subparallel with the ground surface at about 5° from horizontal.

The intent of the analyses of these representative landslides is to determine the probable conditions leading to failure. Thus, we analyze both slides in static (aseismic) conditions to determine the likelihood of failure caused by changes in ground-water conditions in the absence of earthquake shaking. We then analyze both slides in dynamic (seismic) conditions to determine if failure would have occurred in earthquake shaking similar to that produced in 1811–12. If the analyses show that (1) the bluffs are stable in aseismic conditions even in the worst conceivable ground-water conditions and (2) the bluffs would fail catastrophically in severe earthquake shaking, then we can conclude that these landslides did indeed form as a result of the 1811–12 earthquakes.

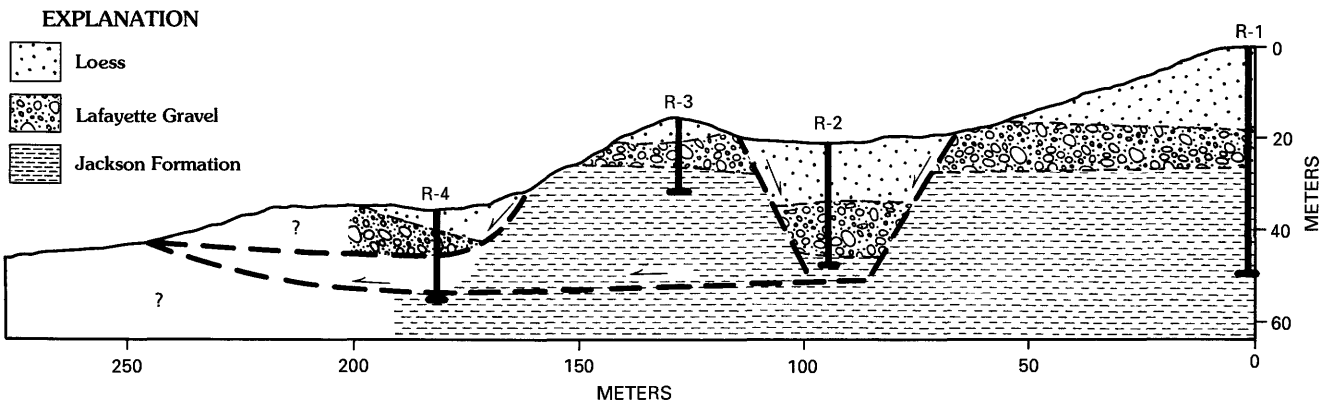

Figure 5. Profile of Stewart landslide showing subsurface stratigraphy (from drill holes shown on fig. 4) and diagrammatic representation of failure surfaces (dashed lines). Intact stratigraphy is shown at R-1.

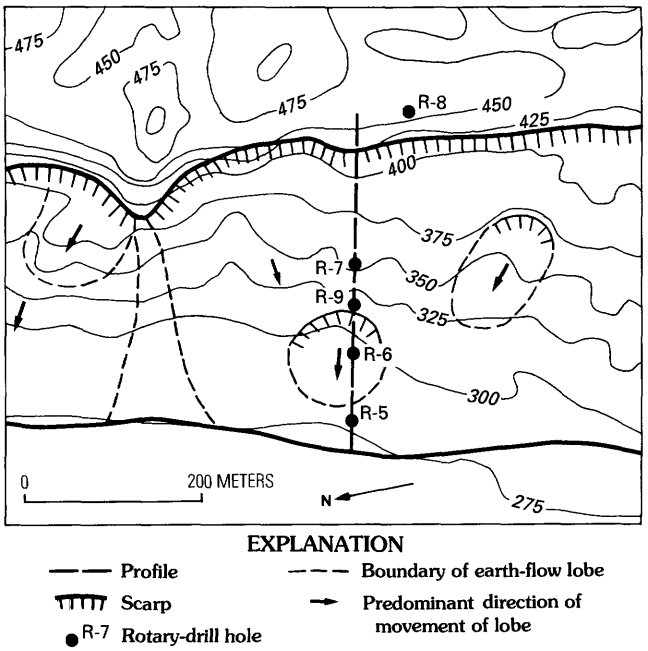

Figure 6. Map of the part of the Campbell earth-flow complex near the line of profile. Contours in feet above mean sea level (1 ft = 0.305 m).

GEOTECHNICAL INVESTIGATION

The purpose of the geotechnical investigation was to procure soil samples and conduct laboratory and in situ engineering tests to determine the soil properties that affect slope stability. Fundamental properties required for stability analyses are unit weight and shear strength of the soil. Index properties such as grain-size distribution, plasticity, water content, and color are determined to classify and correlate soil layers between sample sites.

We drilled nine hollow-stem rotary boreholes on the two landslides from which we procured two types of samples: split-spoon samples from standard-penetration testing (SPT) and 13-cm-diameter undisturbed piston cores. Split-spoon samples are obtained by hammering a steel sampler into the bottom of the borehole; such samples typically are heavily disturbed by the sampling process and are used primarily for determining index properties. Piston cores are procured by carefully pushing a thin-walled steel tube into the bottom of the hole; piston cores provide nearly undisturbed soil samples that are used to measure soil unit weight and shear strength. Additional samples were carved from surface outcrops and obtained by hand augering; these samples were used primarily to determine index properties, but some block samples were of sufficient quality to allow shear-strength testing. A detailed description of the sampling techniques used is given by Jibson (1985).

Soil shear strength commonly is characterized in one of two ways, depending on the conditions being considered (Newmark, 1965; Lambe and Whitman, 1969). In static (aseismic) conditions, drained or effective shear strength is characterized using two components: the angle of internal friction (ϕ') and the cohesion (c'). The pore-water pressure is assumed to be measurable or estimable and is accounted for explicitly in the stability analysis, and no pore-water pressures in excess of hydrostatic are present. In dynamic (seismic) conditions, undrained or total shear-strength parameters are used. During earthquakes, slope materials behave in a so-called undrained manner because excess pore-water pressures induced by dynamic deformation of the soil column cannot dissipate during the relatively brief duration of the shaking. Undrained strength also is called total strength because the respective contributions of friction, cohesion, and pore pressure are not differentiated and the total strength is expressed as a single quantity.

Drained shear strengths of undisturbed soil samples were measured by direct shear and consolidated-undrained (CUTX) triaxial shear (Jibson, 1985). Direct shear tests were run slowly enough to allow full drainage (no excess pore pressure), and the frictional and cohesive components of the shear strength were measured directly under different normal loads. In triaxial tests, no drainage

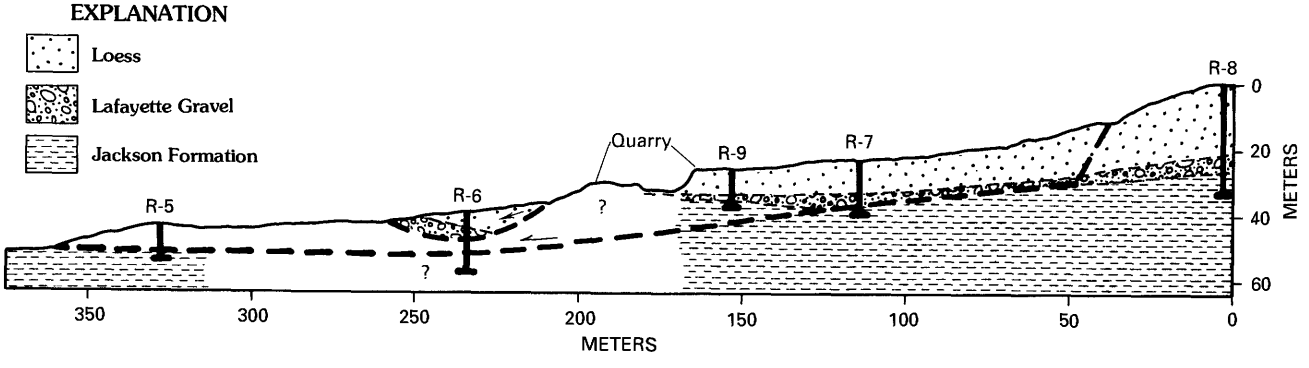

Figure 7. Profile of Campbell landslide showing subsurface stratigraphy (from drill holes shown on fig. 6) and diagrammatic representation of failure surfaces (dashed lines). Intact stratigraphy is shown at R-8.

is allowed, but pore pressures are measured throughout the test and can be mathematically removed from the results to estimate the drained conditions.

Undrained shear strengths were measured primarily by CUTX tests. CUTX results were supplemented by a variety of other methods for measuring undrained strength where undisturbed samples were unavailable; these other methods included vane shear, penetrometer, and correlation with SPT blow counts (Jibson, 1985).

STATIC (ASEISMIC) SLOPE STABILITY ANALYSIS

IDEALIZED PRE-LANDSLIDE BLUFF MODEL

To analyze the long-term stability of the bluffs at the Stewart and Campbell sites, we constructed idealized models of the pre-landslide bluffs for stability analysis. Undisturbed bluffs adjacent to the slides were examined to estimate the pre-landslide slope morphology, and stratigraphic data from the drilling were used to construct detailed profile models of the bluffs for two-dimensional analysis. Geotechnical properties of the stratigraphic layers in the idealized model were assigned using the results of the shear-strength tests; layers where no shear-strength tests were performed were assigned strengths based on stratigraphic and index-property correlation with layers where shear strengths were measured directly (Jibson, 1985).

Figure 8 shows the idealized model of the pre-landslide bluff at the Stewart site in drained conditions; also shown are the unit weight, drained cohesion intercept, and drained friction angle for each layer defined. The bluff is 45 m high as measured from the profile (fig. 5). Undisturbed bluffs adjacent to the Stewart slide slope about 20° and have simple, uniformly sloping faces. The profile can be approximated by two horizontal lines representing the base and top of the bluff connected by a straight line-segment dipping 20° that represents the bluff face. The stratigraphy of the pre-landslide bluff is best illustrated in hole R-1 (fig. 5) because this hole was placed above the scarp of the Stewart slide in intact material. In the plane of the model, the beds are almost horizontal because the bluff faces north, whereas the dip of the Jackson Formation is to the west and is no more than a few degrees. The bluffs in the area have a thin veneer of colluvial loess, but this would have little effect on slope stability, and so the model shows each unit exposed in the bluff face.

Figure 9 shows the model of the pre-landslide bluff in drained conditions for the Campbell site. The intact bluff adjacent to the Campbell slide has an average slope angle of about 15°, and the profile (fig. 7) indicates a bluff height of 55 m. The structure of the bluff at the Campbell site is somewhat different than that at the Stewart site because the strata dip out of the bluff face at about 5°. Fewer layers are defined for the Campbell slide because drilling results indicate that formations at this site are more uniform.

GROUND-WATER CONDITIONS

Lack of published data or observations makes modeling ground-water conditions along the bluffs difficult. Several potential ground-water conditions were analyzed (fig. 10): (1) a water table at the top of the bluff, with seepage along the entire bluff face (the most critical situation), (2) a water table at the top of the Lafayette Gravel, with seepage on the bluff face only below this level, (3) a water table at the top of the Jackson Formation, (4) a water table at the base of the bluffs (the least critical situation), and (5) a water table sloping upward from the base of the bluffs to the top of the Jackson and a second water table perched on the relatively impermeable Jackson Formation that saturates the Lafayette Gravel. The first condition is a more critical situation than can realistically exist

Layer	Unit weight (kN/m^3)	Drained friction angle	Drained cohesion (kPa)
1	19.3	34°	0.25
2	19.6	35°	0.50
3	19.8	30°	0.43
4	22.0	32°	0.32
5	18.1	15°	2.06
6	18.1	20°	1.81
7	17.3	12°	0.71
8	18.1	20°	2.27
9	18.1	15°	2.06
10	18.1	12°	2.52

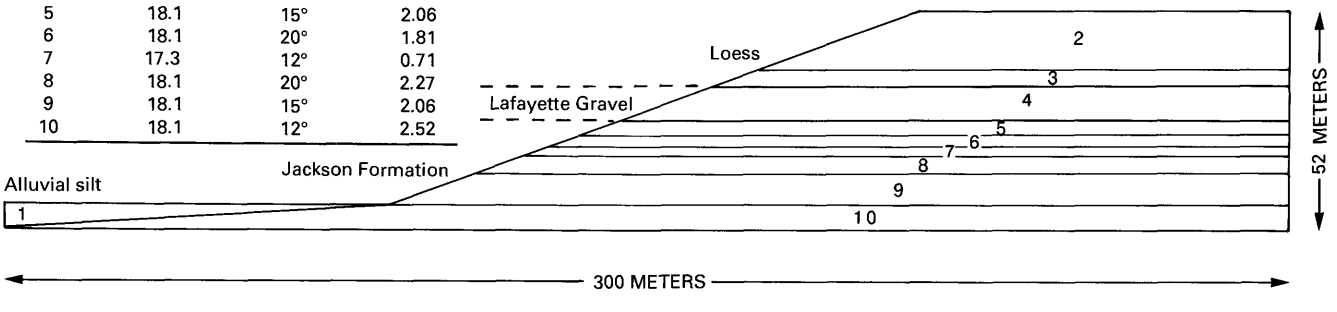

Figure 8. Idealized model of pre-landslide bluff at Stewart site in drained conditions.

Layer	Unit weight (kN/m³)	Drained friction angle	Drained cohesion (kPa)
1	19.3	34°	0.25
2	19.6	35°	0.50
3	19.8	30°	0.43
4	22.0	32°	0.32
5	17.3	20°	0.50
6	18.1	26°	1.51
7	18.1	22°	1.01

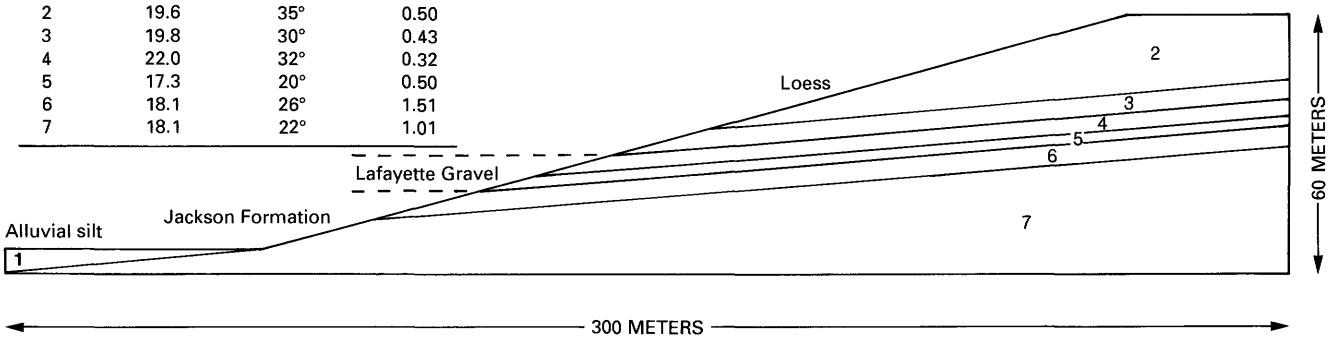

Figure 9. Idealized model of pre-landslide bluff at Campbell site in drained conditions.

in the bluffs and thus provides a worst-case bounding condition. Local hydrologists and geologists who have studied ground-water conditions in the area and who have unpublished water-level data from wells along the bluffs (Robert Davis, Army Corps of Engineers, Memphis District, oral commun., 1983; William Parks, U.S. Geological Survey, Memphis, oral commun., 1983) indicate that condition five is the most likely.

METHOD OF STABILITY ANALYSIS

We used the computer program STABL (Siegel, 1978) to determine the stability of the modeled bluffs in aseismic conditions. STABL randomly generates any number of circular, wedge-shaped, or irregular slip surfaces of any given geometry and calculates the factor of safety[1] for each randomly generated surface. The program plots the 10 most critical surfaces of each given type along with their factors of safety. STABL also calculates safety factors for slip surfaces having predetermined geometries.

[1] The factor of safety (FS) is the ratio of the sum of the resisting forces that act to inhibit slope movement to the sum of the driving forces that tend to cause movement. Slopes having factors of safety greater than 1.0 are thus stable; those having factors of safety less than 1.0 should move.

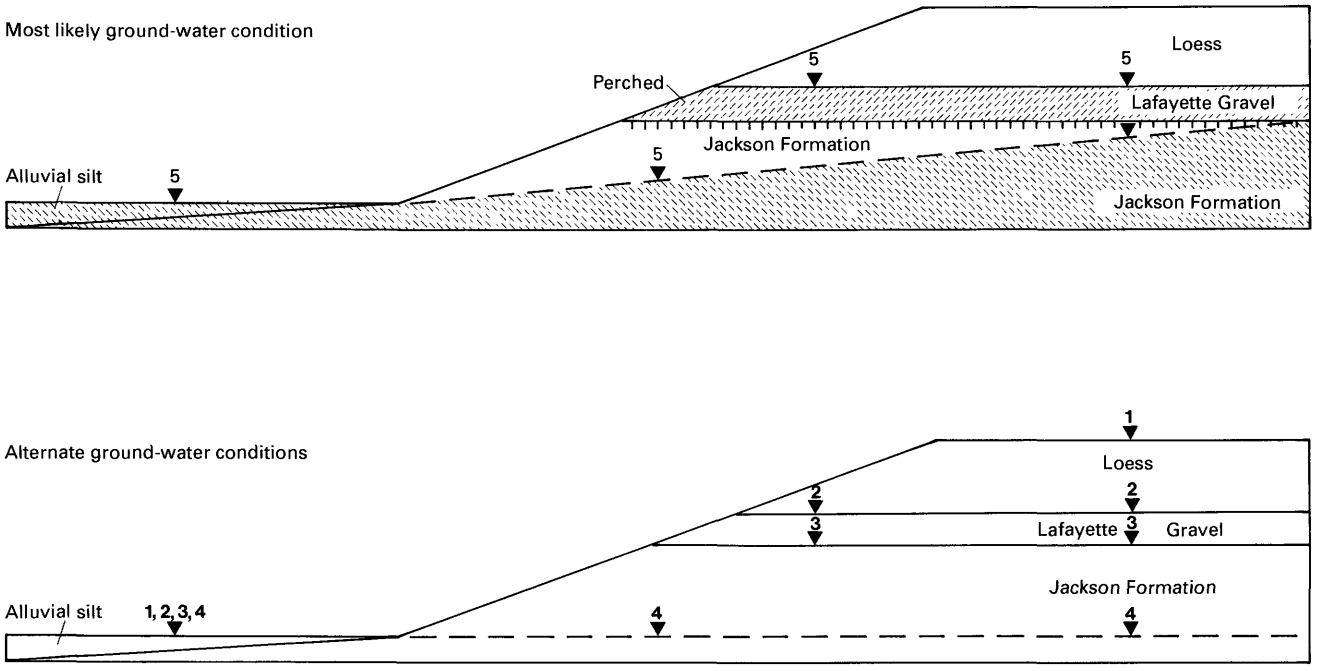

Figure 10. Ground-water conditions modeled in the slope stability analysis. Upper drawing shows most likely ground-water conditions; pattern indicates saturated strata. Lower drawing shows four other possible ground-water conditions. Inverted triangles indicate piezometric surfaces for various ground-water conditions (1–5) described in text.

The locations of the actual failure surfaces were estimated from drilling data and from the surface geometry of the landslides; safety factors were calculated for these surfaces in each ground-water scenario. STABL generated a wide variety of circular and irregular surfaces, and wedge-shaped surfaces were generated in each of the layers in the Jackson Formation and Lafayette Gravel because the landslide geometries and the drilling data indicate that the basal shear surfaces are beneath the loess.

RESULTS OF STATIC SLOPE STABILITY ANALYSIS

Determining the stability of the bluff from the factor of safety (FS) requires some judgment. Gedney and Weber (1978) recommend that engineered slopes have safety factors between 1.25 and 1.50. We use this range as the criterion to evaluate slope stability: between FS 1.00 and 1.25, slopes are considered marginally stable; between FS 1.25 and 1.50, slopes are considered stable; and above FS 1.50, slopes are considered very stable.

Results of the drained stability analyses of the Stewart and Campbell landslides are summarized in table 1. For the Stewart site, the lowest factor of safety in the most critical ground-water situation is 1.32, which indicates that the bluff there is stable in aseismic conditions even in the most critical ground-water condition. In the most likely ground-water condition, the minimum factor of safety at the Stewart site is 1.82: the bluff is very stable. The factor of safety of the observed failure surface in the most likely ground-water condition is 1.88. For the Campbell site, the minimum factor of safety in the most critical ground-water situation is 1.30, also in the stable range. In the most likely ground-water situation, the minimum factor of safety is 2.05, in the very stable range.

Figures 11 and 12 show the effects of ground-water level on factor of safety for differently shaped failure surfaces for the Stewart and Campbell slides, respectively. Visual extrapolation of the lines shows that an artesian piezometric surface tens of meters above ground level at the top of the bluff would be needed to reduce the factor of safety to 1.0 at both sites. Such an artesian condition is implausible because (1) the regional geology and topography preclude such a condition and (2) a piezometric surface far above the bluff top that dips steeply to the bluff base is physically unrealistic. Thus, the Stewart and Campbell landslides could not have formed aseismically in any conceivable ground-water condition.

Figures 13 and 14 show, for the Stewart and Campbell sites, respectively, the locations of the most critical slip surfaces of various shapes and of the observed slip surfaces. For the Stewart site, all the surfaces have grossly similar shapes, but the randomly generated

Table 1. Static factors of safety from stability analyses of the Stewart and Campbell landslides in drained conditions.

[Most critical surface for each ground-water condition shown in bold type]

Type of failure surface	Location of piezometric surface: Base of bluff	Top of Jackson Fm.	Top of Lafayette Gravel	Top of bluff	Sloped and perched
Stewart landslide					
Circular	**1.90**	**1.66**	**1.61**	1.35	**1.82**
Irregular	1.95	1.69	1.64	**1.32**	1.87
Wedge, layer 5	4.06	3.98	3.76	2.83	4.03
Wedge, layer 6	4.24	4.03	3.80	2.79	4.23
Wedge, layer 7	2.46	2.28	2.14	1.47	2.45
Wedge, layer 8	3.81	3.39	3.23	2.51	3.72
Wedge, layer 9	2.83	2.48	2.38	1.88	2.71
Wedge, layer 10	2.40	2.10	2.03	1.68	2.25
Observed surface	1.96	1.73	1.67	1.40	1.88
Campbell landslide					
Circular	**2.33**	**1.77**	**1.66**	1.35	**2.05**
Irregular	2.40	1.82	1.71	1.35	
Wedge, layer 5	2.44	2.40	2.17	**1.30**	2.41
Wedge, layer 6	3.32	2.99	2.78	1.96	3.33
Wedge, layer 7	2.41	1.87	1.76	1.32	2.09
Observed surface	2.88	2.86	2.60	1.53	2.75

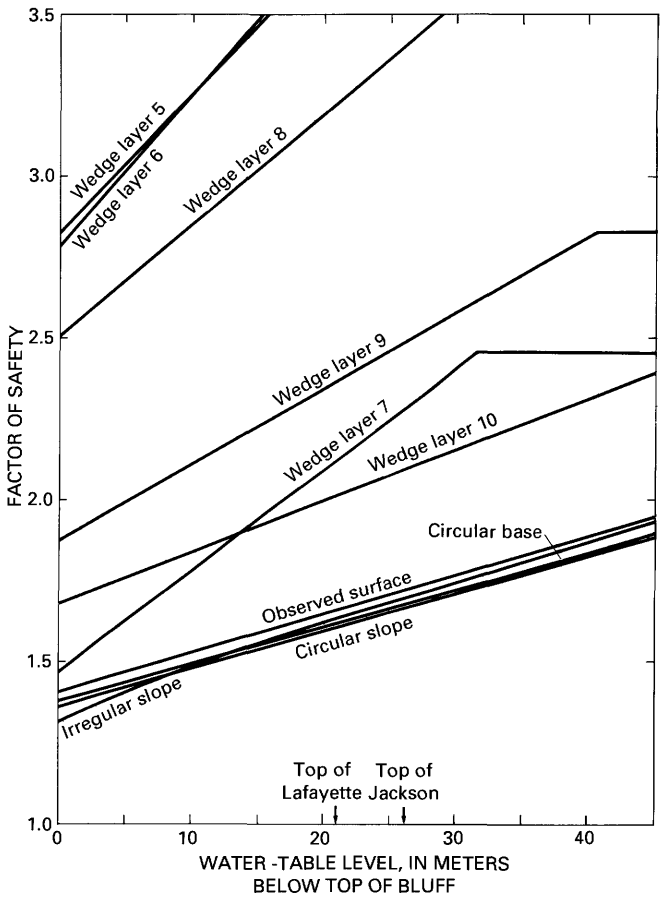

Figure 11. Static, drained factor of safety versus water-table level for several failure geometries at the Stewart site.

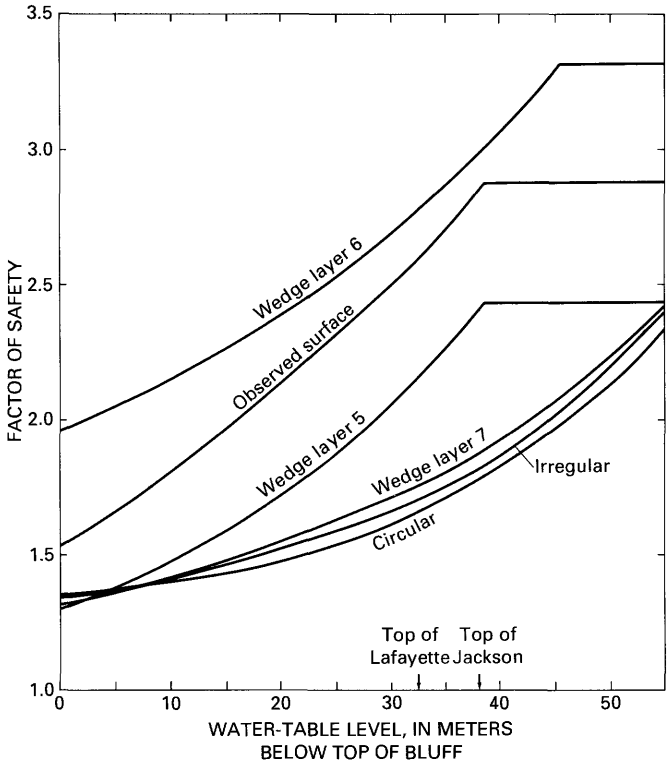

Figure 12. Static, drained factor of safety versus water-table level for several failure geometries at the Campbell site.

surfaces all lie well above the observed failure surface. For the Campbell site, the two most critical slip surfaces lie well below the observed surface and have factors of safety much lower than the observed surface and its adjacent randomly generated surface. This disparity between the most critical randomly generated slip surfaces and the observed surfaces further confirms that the existing landslides at the Stewart and Campbell sites did not form in aseismic, drained conditions.

DYNAMIC (SEISMIC) SLOPE STABILITY ANALYSIS

We use the dynamic displacement analysis developed by Newmark (1965), now used widely in engineering practice (Seed, 1979), to evaluate the seismic stability of the bluffs. Newmark's method models a landslide as a rigid friction block of known critical acceleration—the acceleration required to overcome frictional resistance and initiate sliding—on an inclined plane. The analysis calculates the cumulative displacement of the block as it is subjected to the effects of an earthquake acceleration-time history, and the user judges the significance of the displacement.

Laboratory model tests (Goodman and Seed, 1966) and analysis of earthquake-induced landslides (Wilson and Keefer, 1983) confirm that Newmark's method fairly accurately predicts slope displacements if slope geometry and soil properties are known and earthquake ground accelerations can be estimated. Newmark's method is a significant improvement over traditional pseudostatic stability analysis, which defines any exceedence of the critical acceleration, no matter how brief, as failure.

Newmark (1965) showed that the critical acceleration is a function of the static factor of safety and the landslide geometry:

$$a_c=(FS-1)g \sin \alpha \qquad (1)$$

where

a_c is the critical acceleration in terms of g, the acceleration due to Earth's gravity;

FS is the static factor of safety; and

α is the angle (herein called the thrust angle) from the horizontal that the center of mass of the potential landslide block first moves.

We used an algorithm to apply Newmark's method that is similar to that described by Wilson and Keefer (1983). Figure 15*A* shows a strong-motion record having a hypothetical a_c of 0.2 g superimposed. To the left of

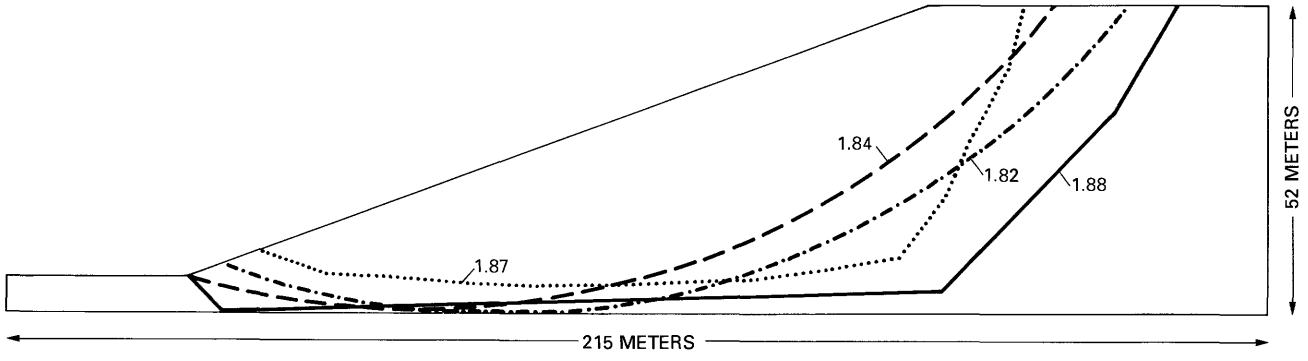

Figure 13. Critical slip surfaces and their factors of safety for static, drained conditions at the Stewart site for the most likely groundwater condition. Solid line is actual failure surface.

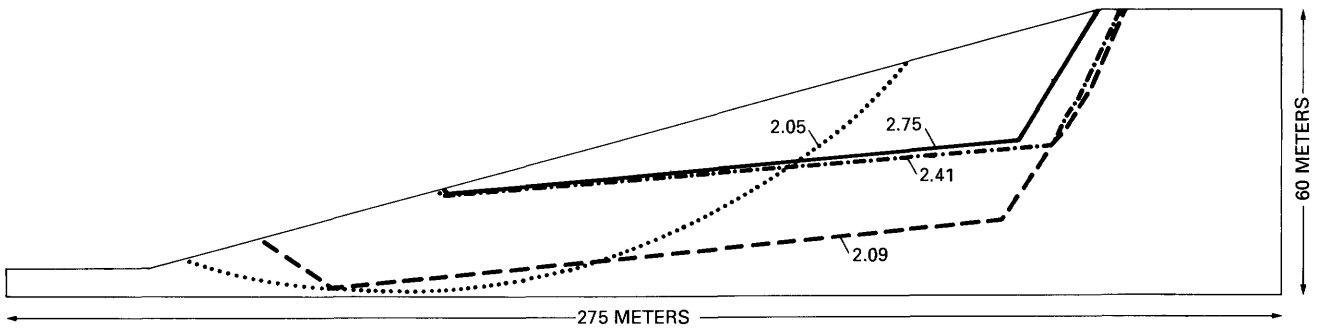

Figure 14. Critical slip surfaces and their factors of safety for static, drained conditions at the Campbell site for the most likely ground-water condition. Solid line is actual failure surface.

point X (fig. 15), the accelerations are less than a_c, and no landslide displacement occurs. To the right of point X, those parts of the strong-motion record lying above a_c are integrated over time to derive a velocity profile of the block. Integration begins at point X (figs. 15*A*, *B*), and the velocity increases to point Y, the peak velocity for this pulse. Past point Y, the ground acceleration drops below a_c, but the block continues moving because of its inertia. Friction and ground motion in the opposite direction cause the block to decelerate until it stops at point Z. All pulses of ground motion exceeding a_c are similarly integrated to yield a velocity profile (fig. 15*B*), which, in turn, is integrated to yield the cumulative displacement of the block (fig. 15*C*).

For simplicity, we modified the algorithm of Wilson and Keefer (1983) to prohibit upslope displacement. This prohibition was justified by Newmark (1965), as well as other investigators (Franklin and Chang, 1977; Chang and others, 1984; Lin and Whitman, 1986), because the resistance of a slope to sliding is highly asymmetrical: a_c in the upslope direction is generally so much greater than a_c in the downslope direction that it can be assumed to be infinitely large. In most cases, the upslope a_c is greater than the peak earthquake acceleration, and no error is introduced by prohibiting upslope displacement.

Conducting a Newmark analysis requires three pieces of information: the static factor of safety and the thrust angle of the potential landslide, both needed to calculate the critical acceleration, and an earthquake acceleration-time history.

FACTOR OF SAFETY

During earthquakes, slope materials behave in a so-called undrained manner; thus, layered models of the bluffs in undrained conditions were constructed. Because undrained shear strength depends in large part on consolidation stress, layers of roughly similar thickness were constructed that reflect the increase in shear strength with depth even for relatively homogeneous materials.

Different shear-strength parameters were used for various layers depending on the ground-water conditions. For the Lafayette Gravel and the Pleistocene loess, drained strengths were used above the water table, undrained strengths below the water table. The Jackson Formation was considered saturated in all conditions because of its high clay content and consequent low permeability, and undrained shear strengths were used in all cases. The high

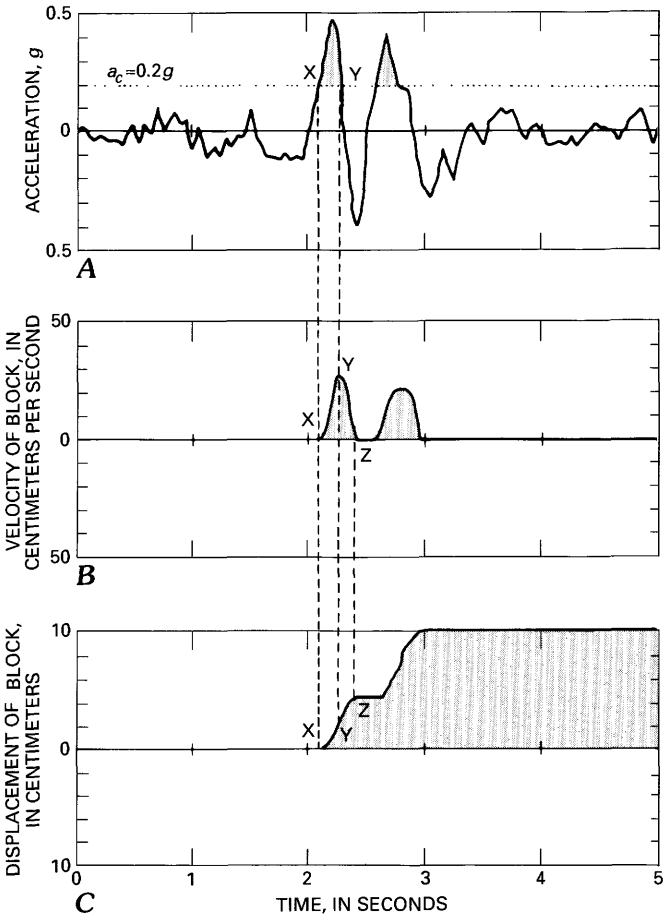

Figure 15. Demonstration of the Newmark-analysis algorithm (adapted from Wilson and Keefer, 1983). Points X, Y, and Z are discussed in text. *A*, Strong-motion record with critical acceleration (dotted line) superimposed. *B*, Velocity of landslide block versus time. *C*, Displacement of block versus time.

Layer	Unit weight (kN/m^3)	Undrained shear strength (kPa)
1	19.3	8.41
2	19.6	4.63
3	19.6	16.01
4	19.6	4.63
5	22.0	3.93
6	22.0	4.46
7	18.1	2.54
8	18.1	3.58
9	17.3	2.42
10	18.1	5.04
11	18.1	3.17
12	18.1	3.78
13	18.1	4.38

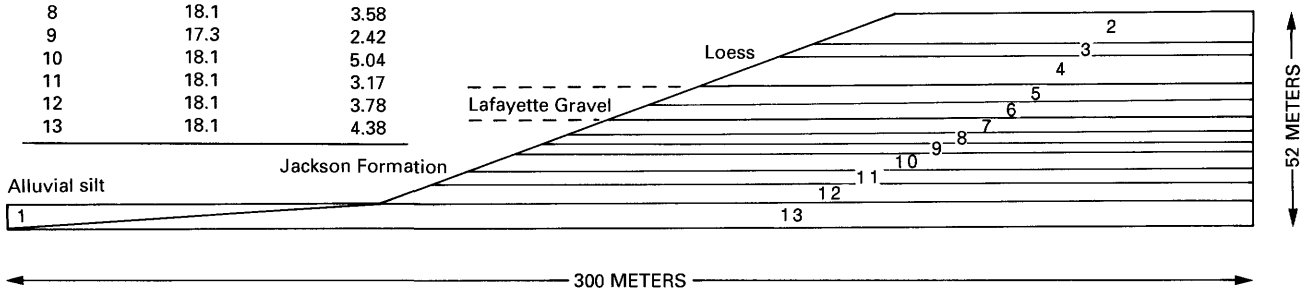

Figure 16. Idealized model of pre-landslide bluff at Stewart site in undrained conditions.

undrained shear strength of the cemented loess layer makes the situation where the water table is at the top of the bluffs less critical than other situations.

STABL was used to generate potential failure surfaces and to determine the most critical failure surfaces in the same manner as described above for the drained stability analysis. Figures 16 and 17 show the undrained bluff models for the Stewart and Campbell sites, respectively; unit weights and undrained shear strengths for each layer are shown. Table 2 summarizes the results of the undrained stability analyses. The lowest factors of safety for the Stewart and Campbell sites are 1.53 and 1.32, respectively; both bluffs were statically stable in undrained conditions.

Figures 18 and 19 show the locations of the critical undrained failure surfaces for the Stewart and Campbell sites, respectively, in the most likely ground-water condition. For the Campbell slide, the most critical surface, a wedge failure in layer five, coincides almost exactly with the observed failure surface. For the Stewart slide, all the slip surfaces, including the observed failure surface, plot very close to one another and have similar factors of safety. Both circular surfaces have large radii and approximate planar basal shear surfaces. The landslide geometry suggests (fig. 5) that translatory movement likely occurred along a weak layer within the Jackson Formation; thus, a wedge failure in one of the deeper layers might have been expected to produce the lowest factor of safety. A thin, weaker layer that was not detected in the drill holes may exist in the Jackson Formation along which sliding occurred, but the close proximity of the observed failure surface to the most critical surfaces generated by STABL indicates that the model generally agrees with observations.

Layer	Unit weight (kN/m^3)	Undrained shear strength (kPa)
1	19.3	8.41
2	19.6	16.01
3	19.8	4.63
4	22.0	4.33
5	17.3	1.26
6	18.1	2.87
7	18.1	3.40
8	18.1	3.75
9	18.1	4.10

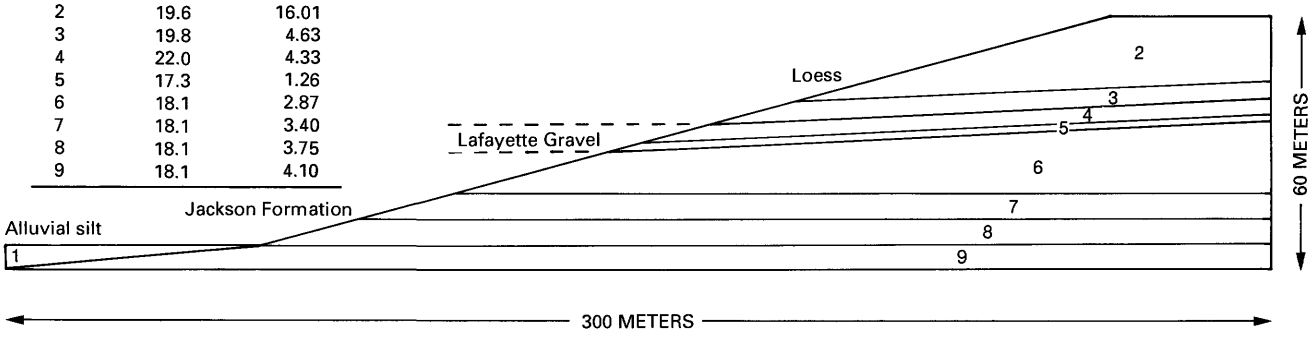

Figure 17. Idealized model of pre-landslide bluff at Campbell site in undrained conditions.

Table 2. Static factors of safety from stability analyses of the Stewart and Campbell landslides in undrained conditions.

[Most critical surface for each ground-water condition shown in bold type]

Type of failure surface	Location of piezometric surface				
	Base of bluff	Top of Jackson Fm.	Top of Lafayette Gravel	Top of bluff	Sloped and perched
Stewart landslide					
Circular	1.72	1.72	1.64	**1.99**	1.62
Irregular	**1.64**	**1.64**	**1.55**	2.16	**1.53**
Wedge, layer 5	2.81	2.81	2.50	3.59	2.49
Wedge, layer 6	3.23	3.23	2.96	3.84	2.93
Wedge, layer 7	2.19	2.19	1.99	2.81	1.97
Wedge, layer 8	3.18	3.18	3.05	3.57	3.02
Wedge, layer 9	2.00	2.00	1.89	2.41	1.87
Wedge, layer 10	1.99	1.99	1.88	2.25	1.87
Observed surface	1.74	1.74	1.66	2.12	1.65
Campbell landslide					
Circular	1.90	1.90	1.79	2.55	1.79
Irregular	1.79	1.79	1.74	3.12	1.74
Wedge, layer 5	**1.44**	**1.44**	**1.32**	3.68	**1.32**
Wedge, layer 6	1.85	1.85	1.76	3.19	1.76
Wedge, layer 7	1.84	1.84	1.77	2.97	1.77
Wedge, layer 8	1.76	1.76	1.71	2.60	1.71
Wedge, layer 9	1.67	1.67	1.64	**2.39**	1.64
Observed surface	2.63	2.63	1.57	5.64	1.57

The fact that the most critical computer-generated surfaces closely parallel the observed failure surfaces indicates that the bluff models are realistic and that the bluffs at the Stewart and Campbell sites probably failed in undrained conditions.

THRUST ANGLE

The thrust angle is the direction the center of gravity of the slide mass moves when displacement first occurs. For a planar slip surface parallel with the slope face (an infinite slope), this angle is the slope angle. For rotational movement, Newmark (1965) showed that the thrust angle is the angle between the vertical and a line segment connecting the center of gravity of the slide mass and the center of the slip circle.

Figure 18 shows geometric constructions of the thrust angles of the most critical surfaces for the Stewart slide. Thrust angles for these surfaces all are 15°–16°. The thrust angle of the observed surface is difficult to estimate because of the irregular shape of the surface and the consequent complex movement. We calculated an average inclination for the observed failure surface by weighting the inclinations of the line segments forming the observed surface by their relative lengths. This yields an average inclination of 16°, consistent with that of the other generated surfaces.

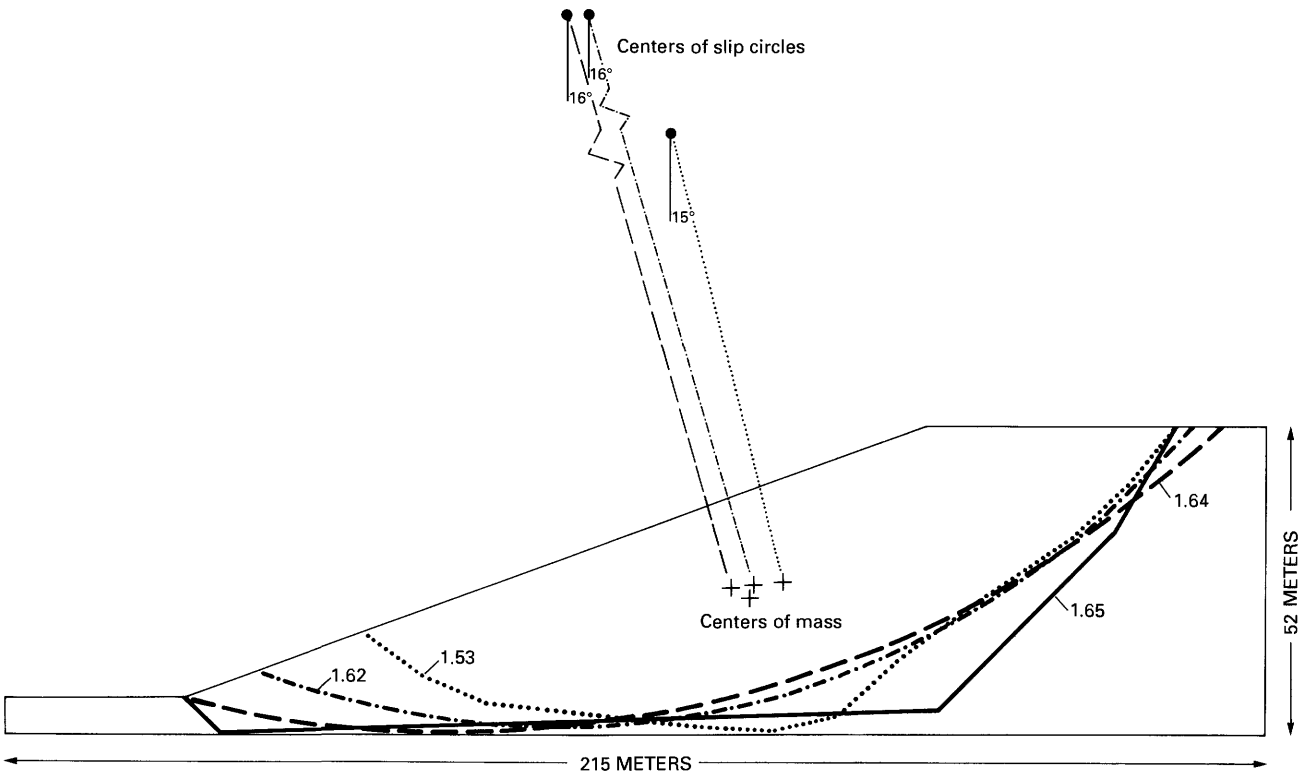

Figure 18. Critical slip surfaces and their factors of safety in static, undrained conditions at the Stewart site for the most likely groundwater condition. Geometric construction to determine the thrust angle is shown. Solid line is actual failure surface.

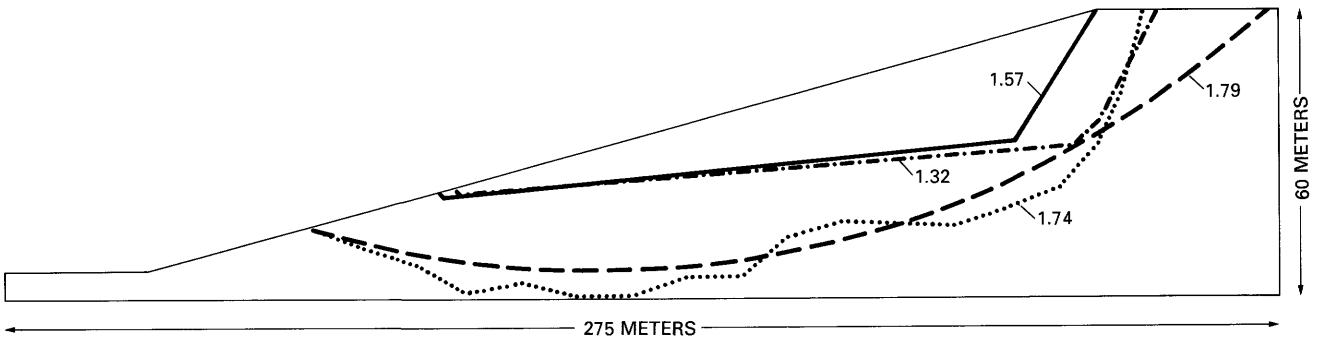

Figure 19. Critical slip surfaces and their factors of safety in static, undrained conditions at the Campbell site for the most likely ground-water condition. Solid line is actual failure surface.

For the Campbell slide, the thrust angle is the inclination of the basal shear surface along which sliding occurred in layer five. The simple morphology of the slide and the coincidence of the most critical slip surface with the observed one justify this approach. Layer five dips 5°; this is used as the thrust angle.

EARTHQUAKE ACCELERATION-TIME HISTORY

Choosing a strong-motion record to represent the ground motions from the 1811–12 earthquakes is difficult because most available records are for California earthquakes, which probably differ in many respects from large earthquakes in the Central United States (e.g., Nuttli, 1983). Differences in the propagation of strong ground motion, however, may not be as great as previously believed and appear to be significant only at great epicentral distances (>150 km) for very large earthquakes (Hanks and Johnston, 1992). Estimating ground-motion characteristics of the 1811–12 earthquakes at the Stewart and Campbell sites and comparing these estimates with existing earthquake records provides a basis for choosing an input ground motion. Peak ground acceleration (PGA), duration, and shaking intensity are used for this comparison, as described below.

Nuttli and Herrmann (1984) used instrumental data from several Central U.S. earthquakes to develop the following equation to relate mean horizontal PGA for soil sites in the Central United States to earthquake magnitude and source distance:

$$\log \hat{a}=0.57+0.50\, m_b-0.83 \log(R^2+h^2)^{1/2}-0.00069\, R \quad (2)$$

where

$\hat{a}$ is the PGA in centimeters per second squared,
m_b is the body-wave magnitude,
R is the epicentral distance in kilometers, and
h is the focal depth in kilometers.

For the 23 January and 7 February 1812 earthquakes, Nuttli's (1973) estimated epicenters (see fig. 1) and magnitudes (m_b 7.1 and 7.4, respectively) are used to calculate epicentral distance. For the 16 December 1811 earthquake, Obermeier's (1989) analysis of the distribution of earthquake-triggered liquefaction effects indicates an epicenter about 15 km southwest of Nuttli's estimated location; we use this location and Nuttli's (1973) estimated magnitude (m_b 7.2). We use 20 km, the approximate maximum depth of instrumentally recorded earthquakes in the seismic zone, for the focal depth. These input parameters yield PGA values at the Stewart and Campbell sites between about 0.4 g and 0.7 g (table 3).

PGA measures only a single point (the maximum acceleration, of whatever frequency) in an acceleration-time history and is thus a rather crude single measure of earthquake shaking intensity. A more comprehensive and quantitative measure of total shaking intensity developed by Arias (1970) is useful in seismic-hazard analysis and correlates well with the distribution of earthquake-induced landslides (Harp and Wilson, 1989). Arias intensity is the integral over time of the square of the acceleration, expressed as

$$I_a=\pi/2g \int[a(t)]^2 dt \quad (3)$$

where

I_a is the Arias intensity, expressed in units of velocity, and
$a(t)$ is the ground acceleration as a function of time.

Wilson and Keefer (1985) developed a simple relationship between Arias intensity, earthquake magnitude, and source distance:

$$\log I_a=M-2\log R-4.1 \quad (4)$$

where

I_a is in meters per second,
M is moment magnitude, and
R is earthquake source distance in kilometers.

Equation 4 was developed from California earthquakes and may underestimate the shaking intensity in the Central United States. Table 3 shows Arias intensities

Table 3. Strong-motion records used to model ground shaking from the 1811–12 earthquakes at the Stewart and Campbell landslides.

[Characteristics of the 1811–12 earthquakes estimated as described in text. All strong-motion records are from U.S. Geological Survey recording stations except for the Tabas, Iran, record (Hadley and others, 1983). M is moment magnitude (estimates for the 1811–12 earthquakes from Hamilton and Johnston, 1990); $\hat{a}$ is peak ground acceleration; T is duration of strong shaking as defined by Dobry and others (1978); I_a is Arias (1970) intensity; D_N is Newmark (1965) displacement (range shown covers range of critical accelerations discussed in text)]

Earthquake Recording site, component	M	R (km)	$\hat{a}$ (g)	T (s)	I_a (m/s)	D_N (cm)
Stewart landslide						
16 Dec 1811, New Madrid, Mo., Stewart landslide site (estimated)	8.2	68	0.39	20–40	2.7* 2.7–5.5†	
15 Oct 1979, Imperial Valley, Calif., El Centro differential array, 360°	6.5	7	0.49	6.6	2.1	6–8
24 Nov 1987, Superstition Hills, Calif., Superstition Mountain site 8, 135°	6.5	6	0.90	12.2	6.8	23–25
23 Jan 1812, New Madrid, Mo., Stewart landslide site (estimated)	8.1	24	0.74	18–40	17.4* 8.9–19.7†	
9 Feb 1971, San Fernando, Calif., Pacoima Dam, 164°	6.6	3	1.22	6.7	9.1	50–55
16 Sept 1978, Tabas, Iran, 74°	7.4	3	0.71	16.1	10.0	39–44
7 Feb 1812, New Madrid, Mo., Stewart landslide site (estimated)	8.3	44	0.71	25–40	8.2* 11.3–18.1†	
24 Nov 1987, Superstition Hills, Calif., Superstition Mountain site 8, 135°	6.5	6	0.90	12.2	6.8	23–25
16 Sept 1978 Tabas, Iran, 74°	7.4	3	0.71	16.1	10.0	39–44
Campbell landslide						
16 Dec 1811, New Madrid, Mo., Campbell landslide site (estimated)	8.2	59	0.44	20–40	3.6* 3.5–7.0†	
24 Nov 1987, Superstition Hills, Calif., Parachute test site, 315°	6.5	1	0.52	10.9	3.0	124–206
24 Nov 1987, Superstition Hills, Calif., Superstition Mountain site 8, 135°	6.5	6	0.90	12.2	6.8	137–215
23 Jan 1812, New Madrid, Mo., Campbell landslide site (estimated)	8.1	27	0.70	18–40	13.7* 7.9–17.6†	
24 Nov 1987, Superstition Hills, Calif., Superstition Mountain site 8, 135°	6.5	6	0.90	12.2	6.8	137–215
16 Sept 1978, Tabas, Iran, 74°	7.4	3	0.71	16.1	10.0	278–486
7 Feb 1812, New Madrid, Mo., Campbell landslide site (estimated)	8.3	49	0.65	25–40	6.6* 9.5–15.2†	
24 Nov 1987, Superstition Hills, Calif., Superstition Mountain site 8, 135°	6.5	6	0.90	12.2	6.8	137–215
16 Sept 1978, Tabas, Iran, 74°	7.4	3	0.71	16.1	10.0	278–486

* Estimated using equation 4.
† Estimated using equation 5.

estimated from equation 4 using moment-magnitude estimates from Hamilton and Johnston (1990) and source distances based on earthquake locations as described above.

Arias intensity also correlates closely with the combination of PGA and duration. R.C. Wilson (U.S. Geological Survey, written commun., 1988) developed an empirical

equation using 43 strong-motion records to predict Arias intensity from PGA and a specific measure of duration:

$$I_a=0.9\,T\hat{a}^2 \quad (5)$$

where

I_a is in meters per second,
$\hat{a}$ is the peak ground acceleration in g's, and
T is the duration (hereafter called Dobry duration) in seconds, defined by Dobry and others (1978) as the time required to build up the central 90 percent of the Arias intensity.

Estimating Arias intensities from the 1811–12 earthquakes using this method requires an estimate of the duration of strong shaking.

Because duration is a difficult parameter to estimate, we use a variety of methods and compare the results to estimate a probable range of durations of strong shaking. Dobry and others (1978) proposed an empirical relationship between duration and magnitude:

$$\log T=0.432M-1.83 \quad (6)$$

where

T is Dobry duration in seconds, and
M is unspecified earthquake magnitude (probably local magnitude, M_L).

In the magnitude range of interest, M_L values are about 0.1 magnitude points greater than m_b values. Thus, equation 6 yields Dobry durations of 20, 18, and 25 s, respectively, for the three 1811–12 earthquakes (table 3).

Krinitzsky and Marcuson (1983) plotted bracketed durations (time between first and last acceleration pulses above 0.05 g) against MMI for different site conditions. Although few data plot in the MMI X–XI range of interest here, their curves suggest a bracketed duration between 40 and 60 s. Bracketed durations at the 0.05-g level are about 50 percent longer than Dobry durations in the magnitude range of interest (Dobry and others, 1978); thus, the lower value of 40 s is a reasonable estimate of the Dobry duration for all three 1811–12 earthquakes using this method.

We also examined estimated seismic source durations to verify that the ranges estimated above are realistic. Somerville and others (1987) developed theoretical and empirical relationships between earthquake moment and source duration for earthquakes in eastern North America. Using moment estimates for the 1811–12 events of $10^{28.2}$–$10^{28.5}$ dyne-cm (A.C. Johnston, Memphis State University, written commun., 1991) yields source durations of 26–33 s, within the ranges estimated above.

We applied equation 5 to the PGA values and the upper and lower bound durations estimated above to estimate Arias intensities at the Stewart and Campbell sites for the three 1811–12 earthquakes. Resulting Arias intensity estimates are shown in table 3. Estimates for the 16 December 1811 and 23 January 1812 earthquakes using equation 4 are within the range of intensities estimated using equation 5, and intensity estimates for the 7 February 1812 earthquake are somewhat lower. Both methods thus provide compatible intensity estimates that can be used to characterize shaking conditions at the two sites.

Although strong motion has not been recorded for earthquakes in the magnitude range of the 1811–12 events, several existing strong-motion records have shaking characteristics similar enough to estimated shaking characteristics of the 1811–12 events to be useful. We examined an extensive catalog of digitized strong-motion records, primarily from California earthquakes, and selected two records for each site for each of the three 1811–12 earthquakes (a total of six records for each site). Records were selected to match, as closely as possible, the estimated range of Arias intensities and PGA's from the 1811–12 events so as to bracket the likely range of shaking conditions that actually occurred. None of the available strong-motion records have Arias intensities greater than 10 m/s; therefore, where estimated Arias intensities exceed this level, the available record having the greatest Arias intensity is used. Table 3 shows the records selected and compares some of their characteristics with those estimated for the Stewart and Campbell sites from the 1811–12 earthquakes.

CALCULATION OF THE NEWMARK LANDSLIDE DISPLACEMENT

The static factor of safety from the undrained slope stability analysis and the thrust angle from the landslide geometry are combined in equation 1 to calculate the critical acceleration. The critical acceleration is then specified in the computer program that double integrates the strong-motion record to calculate the Newmark displacement.

The significance of the Newmark displacements must be judged in terms of the probable effect on the potential landslide mass. For example, Wieczorek and others (1985) used 5 cm as the critical displacement leading to catastrophic failure of landslides in San Mateo County, Calif.; Keefer and Wilson (1989) used 10 cm as the critical displacement for coherent landslides in southern California. When displacements in this range occur, most soils lose a significant amount of their shear strength and are in a residual-strength condition. Laboratory shear-strength tests on samples from the Stewart and Campbell sites indicate that residual strength is reached after a total shear displacement of about 6 cm (Jibson, 1985); therefore, the 5–10 cm range is reasonable for these landslides. If this amount of displacement is exceeded, static factors of safety using residual shear strengths can be

calculated to determine the stability of the landslide mass after the earthquake shaking (and consequent inertial landslide displacement) ceases.

RESULTS OF DYNAMIC ANALYSIS OF STEWART LANDSLIDE

For the Stewart landslide, we calculated critical accelerations based on a thrust angle of 16° and on the factors of safety of the two circular slip surfaces in the perched and sloped ground-water conditions (FS=1.62, 1.64) because they most closely coincide with the observed surface and have the lowest factors of safety (fig. 18). Equation 1 yields critical accelerations of 0.17–0.18 *g* for these input parameters. Newmark displacements were calculated for these two critical accelerations using the six strong-motion records listed in table 3.

Results of the Newmark analyses are shown in table 3. Displacements are between 6 and 55 cm and thus overlap the critical 5–10 cm range. Displacements generated by the model earthquakes for the 16 December 1811 event are between 6 and 25 cm; in this range, the likelihood of catastrophic failure is uncertain, but enough displacement probably occurred during this earthquake to at least partly reduce soil shear strength and actually reduce the critical acceleration of the slide mass in future earthquakes. The model earthquakes for the 23 January and 7 February 1812 events generated Newmark displacements be tween 23 and 55 cm, amounts that would almost undoubtedly reduce soil shear strengths to residual levels.

Static factors of safety for the Stewart slide were calculated using residual strengths in both drained and undrained conditions (Jibson, 1985), and, in all ground-water conditions, factors of safety were substantially less than 1.0. Therefore, if the soils in the bluff reach residual strength, catastrophic failure will occur even in the absence of earthquake shaking. Because Newmark displacements in successive earthquakes are cumulative, the entire 1811–12 sequence would have generated a minimum of about 1 m of displacement, which certainly would have reduced the strength of the bluff materials to residual levels and caused catastrophic failure.

RESULTS OF DYNAMIC ANALYSIS OF CAMPBELL LANDSLIDE

We computed the Newmark displacement of the Campbell slide using the following input parameters: (1) the static factors of safety from the undrained analysis in the perched and sloped ground-water condition for the observed failure surface (FS=1.57) and the most critical generated surface (FS=1.32) (fig. 19), (2) a thrust angle of 5°, and (3) earthquake acceleration-time histories from table 3. The critical accelerations computed (equation 1) for the two failure surfaces are 0.03 and 0.05 *g*.

Results of the Newmark analysis are shown in table 3. Displacements are between 124 and 486 cm. Such large displacements undoubtedly would lead to reduction of soil shear strength to residual levels. The effect of the much lower critical acceleration of the Campbell slide relative to the Stewart slide is evident in the substantially larger Newmark displacements; any of the earthquakes modeled would generate large inertial displacements that would reduce soil strength to residual levels. Static slope stability analyses using residual strengths in both drained and undrained conditions all yield factors of safety well below 1.0; therefore, catastrophic failure would occur after large earthquake-induced displacements in the slope.

SUMMARY OF STABILITY ANALYSES

The static stability analyses of the Stewart and Campbell landslides show that failure could not have occurred in any conceivable ground-water condition in the absence of earthquake shaking. The dynamic analyses show that earthquake shaking similar to that in 1811–12 would have induced large displacements almost certainly leading to catastrophic failure.

WHAT IF SEISMIC CONDITIONS ARE UNKNOWN?

If we knew nothing about the ground shaking in 1811–12, or if we did not even know if earthquakes had ever occurred in that region, could analysis of these landslides tell us anything of their possible origin? The static stability analyses clearly show that failure in aseismic conditions is highly unlikely, and an earthquake origin could be hypothesized on that basis alone. The dynamic analysis could then be used to estimate the minimum shaking intensities necessary to have caused failure.

Such an approach requires a general relationship between critical acceleration, Arias intensity, and Newmark displacement. To estimate Newmark displacement associated with a given Arias intensity and critical acceleration, we selected 11 strong-motion records having Arias intensities between 0.2 and 10.0 m/s (table 4), which span the range between the smallest shaking intensities that might cause landslide movement and the largest shaking intensities ever recorded. For each strong-motion record, we calculated the Newmark displacement for several critical accelerations between 0.02 and 0.40 *g*, the range of practical interest for earthquake-induced landslides. The resulting data are plotted in figure 20. Data points for each critical acceleration plot fairly linearly in the log-log space of Arias intensity versus Newmark displacement. Best-fit lines from regression models for each value of

Table 4. Strong-motion records selected for analysis.

[M is moment magnitude, $\hat{a}$ is peak ground acceleration, T is duration as defined by Dobry and others (1978), and I_a is Arias intensity. All strong-motion records are from USGS recording stations except for the Tabas, Iran, record (Hadley and others, 1983)]

Earthquake Recording site, component	M	$\hat{a}$ (g)	T (s)	I_a (m/s)
15 Oct 1979, Imperial Valley, Calif., Coachella Canal, station 4, 135°	6.5	0.13	10.4	0.20
6 Aug 1979, Coyote Lake, Calif., Coyote Creek, San Martin, 250°	5.8	0.21	3.8	0.25
21 Jul 1952, Kern County, Calif., Taft School, 111°	7.5	0.14	17.7	0.46
6 Aug 1979, Coyote Lake, Calif., Gilroy array, San Ysidro School, 270°	5.8	0.23	8.5	0.60
15 Oct 1979, Imperial Valley, Calif., Calexico Fire Station, 225°	6.5	0.28	11.1	0.86
1 Oct 1987, Whittier Narrows, Calif., Bulk Mail Center, 280°	6.0	0.45	5.5	1.23
15 Oct 1979, Imperial Valley, Calif., El Centro differential array, 360°	6.5	0.49	6.6	2.12
24 Nov 1987, Superstition Hills, Calif., Parachute test site, 225°	6.5	0.46	10.1	4.15
15 Oct 1979, Imperial Valley, Calif., Bonds Corner, 230°	6.5	0.79	9.8	6.00
9 Feb 1971, San Fernando, Calif., Pacoima Dam, 164°	6.6	1.22	6.7	9.08
16 Sep 1978, Tabas, Iran, 74°	7.4	0.71	16.1	9.96

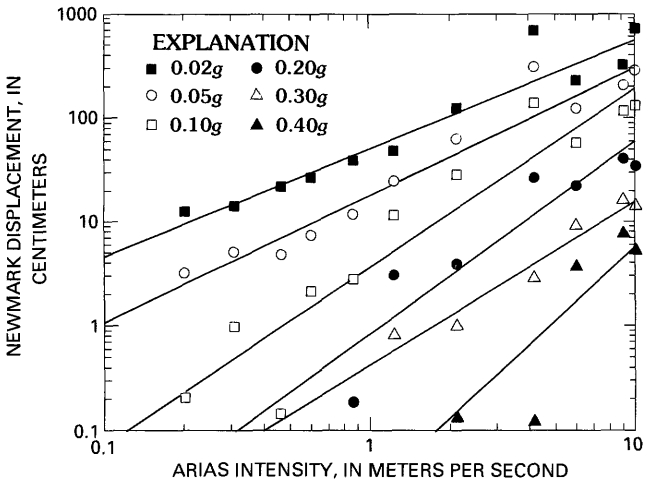

Figure 20. Newmark displacement as a function of Arias intensity for critical accelerations of 0.02–0.40 *g*. Best-fit regression lines for each critical acceleration shown.

critical acceleration have excellent fits (R^2 values between 0.81 and 0.95), and the lines are roughly parallel and proportionately spaced, which suggests that a multivariate

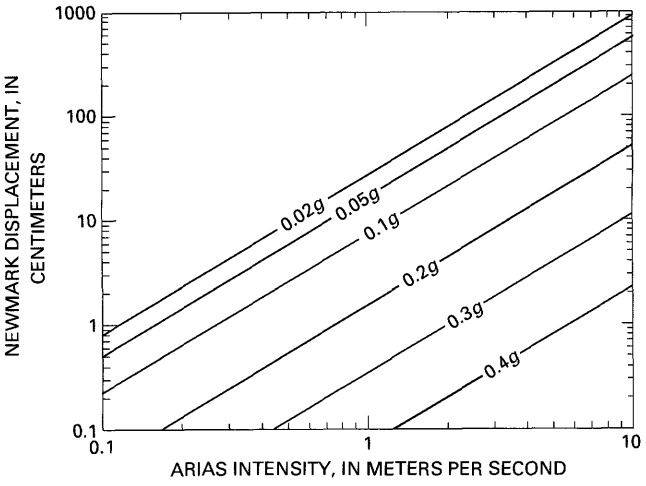

Figure 21. Critical acceleration contours derived from multivariate regression of Arias intensity and critical acceleration versus Newmark displacement (equation 8).

model would fit the data well. Therefore, we constructed a multivariate regression model having the following form:

$$\log D_N = A\log I_a + Ba_c + C \pm \sigma \qquad (7)$$

where

D_N is Newmark displacement in centimeters,
I_a is Arias Intensity in meters per second,
a_c is critical acceleration in *g*'s,
A, B, and C are the regression coefficients, and
σ is the estimated standard deviation of the regression model.

The resulting model has an R^2 of 0.87:

$$\log D_N = 1.460\log I_a - 6.642a_c + 1.546 \pm 0.409 \qquad (8)$$

Figure 21 shows critical acceleration lines derived from equation 8. This model yields the mean value of Newmark displacement when σ is ignored; the variation about this mean, represented by σ, results from the stochastic nature of earthquake ground shaking. Thus, even two strong-motion records having identical Arias intensities can produce significantly different Newmark displacements for slopes having the same critical acceleration.

The threshold earthquake shaking intensity necessary to trigger the Stewart and Campbell landslides can be estimated by judging the amount of Newmark displacement that would reduce shear strength on the failure surface to residual levels and cause catastrophic failure (the critical displacement). As discussed previously, critical displacements of about 10 cm are probably realistic for these types of slides, based on previous studies (Wieczorek and others, 1985; Wilson and Keefer, 1985; Keefer and Wilson, 1989), laboratory shear-strength testing of soil samples from our sites (Jibson, 1985), and field studies of landslides in the

region (Jibson and Keefer, 1988). Inserting a displacement value of 10 cm and the critical accelerations of the Stewart (0.17–0.18 *g*) and Campbell (0.03–0.05 *g*) landslides into equation 8 yields a lower bound Arias intensity of about 2.6 m/s to trigger the Stewart slide and about 0.6 m/s to trigger the Campbell slide.

The threshold earthquake magnitude (M) needed to trigger these landslides can be estimated using equation 4. If we assume a minimum earthquake source distance of 5 km (the focal depth at the epicenter), the Arias intensities estimated above yield lower bound threshold moment magnitudes (**M**) of 5.9 for the Stewart landslide and 5.3 for the Campbell landslide. Lower bound threshold body-wave magnitudes (m_b) can be estimated using equations 2, 5, and 6 in combination, which yield lower bound m_b values of 5.8 for the Stewart slide and 5.4 for the Campbell slide. Although these magnitudes are much smaller than those we believe would have been recorded in 1811–12, they nonetheless provide a lower bound threshold in the absence of any additional information on the seismic shaking.

DISCUSSION

Several damaging earthquakes have occurred in the New Madrid seismic zone since the 1811–12 sequence. Nuttli (1982) described the 20 most damaging events since 1812 and estimated their epicentral locations and body-wave magnitudes. Could any of these more recent earthquakes have triggered the landslides we studied? We answer this question by using equation 8 to estimate the effects from these earthquakes at the Stewart and Campbell landslide sites.

We selected the earthquakes from Nuttli (1982) that would have produced the greatest shaking intensities at the Stewart and Campbell sites. We selected the largest earthquake (m_b=6.2) and then eliminated all earthquakes of lesser magnitudes that were farther from our sites. For earthquakes closer to our sites than the m_b=6.2 event, we selected the next largest magnitude and eliminated all earthquakes of lesser magnitude that were farther from our sites. Using this iterative approach, we selected 3 of the 20 earthquakes that would have produced the greatest shaking intensities at the Stewart and Campbell sites (table 5).

We used equations 4 and 5 to estimate the range of possible Arias intensities that would have been produced from each of these earthquakes at each of our sites. Equation 4 requires the magnitude and distance, which are taken from Nuttli's (1982) estimates. Equation 5 requires knowing the PGA and the duration of strong shaking (defined as previously by Dobry and others, 1978); we estimated the maximum PGA using equation 2 and the duration using equation 6. Table 5 shows characteristics of the three selected earthquakes and the estimated range of PGA's and Arias intensities at the Stewart and Campbell sites. All of the earthquakes would have produced PGA's at the Stewart site much less than the critical acceleration necessary to initiate landslide movement (0.17–0.18 *g*); therefore, none of these earthquakes could have triggered any landslide movement there. At the Campbell site, the PGA's are all at or slightly above the critical acceleration (0.03–0.05 *g*), and thus we need to determine if the estimated Arias intensities would have been sufficient to generate enough displacement to cause catastrophic failure.

Combining the greatest estimated Arias intensity for the Campbell site from table 4 (0.077 m/s) with the range of critical accelerations for the Campbell slide (0.03–0.05 *g*) in equation 8 yields Newmark displacements of 0.4–0.5 cm, an order of magnitude smaller than the critical displacement levels of 5–10 cm required to cause catastrophic failure. Thus, we conclude that no earthquakes since 1812 could have triggered catastrophic movement of the Campbell slide.

Equation 8 and figure 21 can be applied to estimate the dynamic performance of any slope of known critical acceleration because they are derived from generic values of critical acceleration that are not site specific.

Table 5. Most damaging earthquakes since 1811–12.

[m_b is body-wave magnitude from Nuttli (1982); M_L is local magnitude and M is moment magnitude, both converted from m_b as suggested by Heaton and others (1986); *T* is duration estimated from equation 6; *R* is epicentral distance to each site using locations from Nuttli (1982); $\hat{a}$ is peak horizontal ground acceleration estimated from Nuttli and Herrmann (1984); I_a is Arias intensity]

Date	m_b	M_L	M	*T*	Stewart landslide				Campbell landslide			
					R	$\hat{a}$	I_a[1]	I_a[2]	*R*	$\hat{a}$	I_a[1]	I_a[2]
				(s)	(km)	(g)	(m/s)	(m/s)	(km)	(g)	(m/s)	(m/s)
31 Oct 1895	6.2	6.6	6.8	10.5	96	0.09	0.077	0.054	103	0.09	0.077	0.047
4 Nov 1903	5.3	5.6	5.5	3.9	86	0.04	0.006	0.003	94	0.03	0.003	0.003
21 Aug 1905	5.0	5.4	5.4	3.2	75	0.03	0.003	0.004	82	0.03	0.003	0.003

[1] Estimated using equation 4.

[2] Estimated using equation 5.

Thus, several types of regional hazard analyses for earthquake-triggered landslides can be developed using equation 8. A common type of regional earthquake-hazard analysis involves estimating the effects from a proposed model earthquake of given magnitude and location. In such a scenario-based hazard analysis, the seismic stability of slopes of known critical acceleration can be estimated by using (1) equation 4 to estimate the Arias intensity from the postulated earthquake magnitude and location and (2) equation 8 to calculate the Newmark displacement. An alternative approach is to use (1) equation 2 (or a similar attenuation equation appropriate for the region of interest) to estimate the PGA, (2) equation 6 to estimate the duration, (3) equation 5 to calculate the Arias intensity from the PGA and duration, and (4) equation 8 to calculate the Newmark displacement.

In previous applications of the Newmark method to regional seismic-hazard analysis (Wieczorek and others, 1985; Wilson and Keefer, 1985; Keefer and Wilson, 1989), estimates of the amount of Newmark displacement that would result in damaging or catastrophic failure—critical displacements—have been made for different slope materials. As stated previously, critical displacements of 5–10 cm were assigned for materials in San Mateo County, Calif., and other similar materials in southern California. Thus, if critical displacements for slope materials in an area can be estimated using laboratory testing or field observations, then equation 8 can be used to estimate (1) the threshold Arias intensity required to initiate failure of slopes of given critical acceleration and (2) the critical acceleration below which slopes will fail for a given shaking intensity. These approaches can be applied in several ways to estimate regional seismic slope stability. This represents an incremental improvement over the previous methods, which assumed a uniform level of ground shaking throughout a region (Wieczorek and others, 1985).

If the Stewart and Campbell landslides are typical of block slides and earth flows in the New Madrid region, then the shaking-intensity and magnitude thresholds discussed previously could be considered lower bound conditions for triggering large landslides of these types in future earthquakes. Thus, an Arias intensity of about 2.6 m/s, corresponding to a minimum M=5.9 or m_b=5.8 earthquake, would be necessary to trigger block slides similar to the Stewart slide. For earth flows similar to the Campbell slide, an Arias intensity of 0.6 m/s, corresponding to a minimum M=5.3 or m_b=5.4 earthquake, would be required. Obviously, larger earthquakes are required to trigger landslides at greater epicentral distances and across a large area.

In this paper, we have developed and successfully applied a method for determining if a landslide or group of landslides of unknown origin was seismically triggered. An important potential application of this method is in paleoseismology. If a group of landslides in a region can be shown to be statically stable but dynamically unstable, an earthquake origin can be inferred. If such landslide features can be dated, a date for the triggering earthquake can be determined. Dynamic analysis of such landslides can yield minimum shaking intensities that would have been required to trigger failure. In areas such as the Central and Eastern United States, where exposures of recent faults are absent or yield equivocal interpretations, groups of old landslides that can be shown to be triggered by earthquake shaking might be used for paleoseismic dating. If more than one generation of such features exists, earthquake return periods could be established. The possibility of such an application exists in the New Madrid seismic zone, where we (Jibson and Keefer, 1988) have mapped many features of questionable origin, some of which may be an older, more eroded set of landslides.

SUMMARY AND CONCLUSIONS

Static and dynamic analyses of two large landslides that are representative of coherent block slides and earth flows in the New Madrid seismic zone show that neither could have moved in the absence of earthquake shaking, even in unrealistically high ground-water conditions. During earthquake shaking similar to that generated in 1811–12, both would have experienced large displacements leading to catastrophic failure. Analysis of shaking intensities generated by the largest earthquakes since the 1811–12 sequence indicates that no earthquakes since then could have triggered the observed slide movement. Therefore, we conclude that the Stewart and Campbell landslides formed during the 1811–12 earthquakes. These analyses confirm the results of our previous studies (Jibson and Keefer, 1988, 1989) that indicated spatial dependence of the landslides on the locations of the 1811–12 earthquakes.

Back calculations of threshold shaking intensities required to cause catastrophic failure indicate that earthquakes of m_b=5.4 or M=5.3 are required to trigger earth flows similar to the Campbell slide and that earthquakes of m_b=5.8 or M=5.9 are required to trigger coherent slides similar to the Stewart slide.

The method for determining the likely conditions—seismic or aseismic—that triggered failure of these landslides can be applied to landslides in other areas. In some cases, it may impossible to determine an earthquake origin for a landslide or group of landslides if failure in aseismic conditions cannot be ruled out. In cases where an earthquake origin can be demonstrated for a landslide, establishing the age of the sliding will indicate the timing of the triggering earthquake. Back analysis of minimum shaking intensities will establish a lower bound for the triggering

earthquake. Hence, the methods described in this paper can find useful application in paleoseismic studies.

The empirical relationship developed between Newmark displacement, Arias intensity, and critical acceleration also can applied generally to a wide variety of seismic-hazard problems related to slope instability. Specifically, if a model earthquake of designated location and magnitude is postulated, then the Newmark displacement of slopes of known critical acceleration can be estimated. If the critical displacement is known, then the shaking intensity required to cause failure of a slope of known critical acceleration can be estimated, or, for a given shaking intensity, the critical acceleration below which slopes will fail can be determined.

REFERENCES CITED

Arias, A., 1970, A measure of earthquake intensity, *in* Hansen, R.J., ed., Seismic Design for Nuclear Power Plants: Cambridge, Massachusetts Institute of Technology Press, p. 438–483.

Chang, C.J., Chen, W.F., and Yao, J.T.P., 1984, Seismic displacements in slopes by limit analysis: Journal of Geotechnical Engineering, v. 110, p. 860–874

Conrad, T.A., 1856, Observations on the Eocene deposit of Jackson, Miss., with descriptions of 34 new species of shells and corals: Philadelphia Academy of Natural Science, Proceedings, 1855, 1st ser., v. 7, p. 257–258.

Dobry, R., Idriss, I.M., and Ng, E., 1978, Duration characteristics of horizontal components of strong-motion earthquake records: Seismological Society of America Bulletin, v. 68, p. 1487–1520.

Franklin, A.G., and Chang, F.K., 1977, Earthquake resistance of earth and rock-fill dams; Report 5, Permanent displacements of earth embankments by Newmark sliding block analysis: U.S. Army Engineers Waterways Experiment Station Miscellaneous Paper S–71–17, 59 p.

Fuller, M.L., 1912, The New Madrid earthquake: U.S. Geological Survey Bulletin 494, 119 p.

Gedney, D.S., and Weber, W.G., Jr., 1978, Design and construction of soil slopes, *in* Schuster, R.L., and Krizek, R.J., eds., Landslides—Analysis and Control: Transportation Research Board, National Academy of Sciences, Special Report 176, p. 172–191.

Goodman, R.E., and Seed, H.B., 1966, Earthquake-induced displacements in sand embankments: American Society of Civil Engineers, Journal of the Soil Mechanics and Foundation Division, v. 92, no. SM2, p. 125–146.

Hadley, D.M., Hawkins, H.G., and Benuska, K.L., 1983, Strong ground motion record of the 16 September 1978 Tabas, Iran, earthquake: Seismological Society of America Bulletin, v. 73, no. 1, p. 315–320.

Hamilton, R.M., and Johnston, A.C., 1990, Tecumseh's prophecy—Preparing for the next New Madrid earthquake: U.S. Geological Survey Circular 1066, 30 p.

Hanks, T.C., and Johnston, A.C., 1992, Common features of the excitation and propagation of strong ground motion for North American earthquakes: Bulletin of the Seismological Society of America, v. 82, p. 1–23.

Harp, E.L., and Wilson, R.C., 1989, Shaking intensity thresholds for seismically induced landslides [abs.]: Geological Society of America Abstracts with Programs, v. 21, no. 5, p. 90.

Heaton, T.H., Tajima, F., and Mori, A.W., 1986, Estimating ground motions using recorded accelerograms: Surveys in Geophysics, v. 8, p. 25–83.

Jibson, R.W., 1985, Landslides caused by the 1811–12 New Madrid earthquakes: Stanford, Calif., Stanford University, unpub. Ph.D. dissertation, 232 p.

Jibson, R.W., and Keefer, D.K., 1984, Earthquake-induced landslides in the central Mississippi Valley, Tennessee and Kentucky, *in* Gori, P.L., and Hays, W.W., eds., Proceedings of the Symposium on the New Madrid Seismic Zone: U.S. Geological Survey Open-File Report 84-770, p. 353–390.

———1988, Landslides triggered by earthquakes in the central Mississippi Valley, Tennessee and Kentucky: U.S. Geological Survey Professional Paper 1336–C, 24 p.

———1989, Statistical analysis of factors affecting landslide distribution in the New Madrid seismic zone, Tennessee and Kentucky: Engineering Geology, v. 27, p. 509–542.

———1992, Analysis of the seismic origin of a landslide in the New Madrid seismic zone: Seismological Research Letters, v. 63, p. 427–437.

———1993, Analysis of the seismic origin of landslides: Examples from the New Madrid seismic zone: Geological Society of America Bulletin, v. 105, p. 521–536.

Keefer, D.K., and Wilson, R.C., 1989, Predicting earthquake-induced landslides, with emphasis on arid and semi-arid environments, *in* Sadler, P.M., and Morton, D.M, eds., Landslides in a Semi-Arid Environment: Riverside, Calif., Inland Geological Society, v. 2, p. 118–149.

Krinitzsky, E.L., and Marcuson, W.F., III, 1983, Principles for selecting earthquake motions in engineering design: Association of Engineering Geologists Bulletin, v. 20, no. 3, p. 253–265.

Krinitzsky, E.L., and Turnbull, W.J., 1969, Loess deposits of Mississippi: Geological Society of America Special Paper 94, 64 p.

Lambe, T.W., and Whitman, R.V., 1969, Soil Mechanics: New York, John Wiley and Sons, 553 p.

Lin, J.S., and Whitman, R.V., 1986, Earthquake induced displacements of sliding blocks: Journal of Geotechnical Engineering, v. 112, no. 1, p. 44–59.

McGee, W.J., 1891, The Lafayette Formation: U.S. Geological Survey 12th Annual Report, pt. 1, p. 387–521.

———1893, A fossil earthquake: Geological Society of America Bulletin, v. 4, p. 411–414.

Newmark, N.M., 1965, Effects of earthquakes on dams and embankments: Geotechnique, v. 15, no. 2, p. 139–160.

Nuttli, O.W., 1973, The Mississippi Valley earthquakes of 1811 and 1812—Intensities, ground motion, and magnitudes: Seismological Society of America Bulletin, v. 63, p. 227–248.

———1982, Damaging earthquakes of the central Mississippi Valley, *in* McKeown, F.A., and Pakiser, L.C., eds., Investigations of the New Madrid, Missouri, Earthquake

Region: U.S. Geological Survey Professional Paper 1236, p. 15–20.

———1983, Average seismic source-parameter relations for mid-plate earthquakes: Seismological Society of America Bulletin, v. 73, no. 2, p. 519–535.

Nuttli, O.W., and Herrmann, R.B., 1984, Ground motion of Mississippi Valley earthquakes: Journal of Technical Topics in Civil Engineering, v. 110, no. 1, p. 54–69.

Obermeier, S.F., 1989, The New Madrid earthquakes—An engineering-geologic interpretation of relict liquefaction features: U.S. Geological Survey Professional Paper 1336–B, 114 p.

Penick, J.L., 1981, The New Madrid Earthquakes (rev. ed.): Columbia, University of Missouri Press, 176 p.

Potter, P.E., 1955, The petrology and origin of the Lafayette Gravel, part II, geomorphic history: Journal of Geology, v. 63, no. 2, p. 115–132.

Saucier, R.T., 1977, Effects of the New Madrid earthquake series in the Mississippi alluvial valley: U.S. Army Engineers Waterways Experiment Station Soils and Pavements Laboratory, Miscellaneous Paper S–77–5, 25 p.

Seed, H.B., 1979, Considerations in the earthquake-resistant design of earth and rockfill dams: Geotechnique, v. 29, no. 3, p. 215–263.

Siegel, R.A., 1978, STABL User Manual: West Lafayette, Indiana, Purdue University, 104 p.

Somerville, P.G., McLaren, J.P., LeFevre, L.V., Burger, R.W., and Helmberger, D.V., 1987, Comparison of source scaling relations of eastern and western North American earthquakes: Seismological Society of America Bulletin, v. 77, no. 2, p. 322–346.

Stearns, R.G., and Wilson, C.W., 1972, Relationship of earthquakes and geology in west Tennessee and adjacent areas: Tennessee Valley Authority, 128 p.

Varnes, D.J., 1978, Slope movement types and processes, *in* Schuster, R.L., and Krizek, R.J., eds., Landslides—Analysis and Control: Transportation Research Board, National Academy of Science, Special Report 176, p. 11–33.

Wieczorek, G.F., Wilson, R.C., and Harp, E.L., 1985, Map showing slope stability during earthquakes of San Mateo County, California: U.S. Geological Survey Miscellaneous Geologic Investigations Map I–1257E, scale 1:62,500.

Wilson, R.C., and Keefer, D.K., 1983, Dynamic analysis of a slope failure from the 6 August 1979 Coyote Lake, California, earthquake: Seismological Society of America Bulletin, v. 73, no. 3, p. 863–877.

Wilson, R.C., and Keefer, D.K., 1985, Predicting areal limits of earthquake-induced landsliding, *in* Ziony, J.I., ed., Evaluating Earthquake Hazards in the Los Angeles Region—An Earth-Science Perspective: U.S. Geological Survey Professional Paper 1360, p. 316–345.

Published in the Central Region, Denver, Colorado
Manuscript approved for publication August 11, 1993
Edited by Richard W. Scott, Jr.
Graphics prepared by Wayne Hawkins
Photocomposition by Marie Melone

☆ U.S. GOVERNMENT PRINTING OFFICE: 1994-573-038/86018